NASA TECHNICAL MEMORANDUM

NASA TM X-1660

NASA TM X-1660

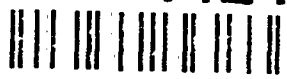

SUBSONIC LONGITUDINAL AERODYNAMIC MEASUREMENTS ON A TRANSPORT MODEL IN TWO SLOTTED TUNNELS DIFFERING IN SIZE

by Arvo A. Luoma, Richard J. Re, and Donald L. Loving

Langley Research Center
Langley Station, Hampton, Va.

NATIONAL AERONAUTICS AND SPACE ADMINISTRATION • WASHINGTON, D. C. • OCTOBER 1968

NASA TM X-1660

SUBSONIC LONGITUDINAL AERODYNAMIC MEASUREMENTS ON A TRANSPORT MODEL IN TWO SLOTTED TUNNELS DIFFERING IN SIZE

By Arvo A. Luoma, Richard J. Re, and Donald L. Loving

Langley Research Center
Langley Station, Hampton, Va.

NATIONAL AERONAUTICS AND SPACE ADMINISTRATION

For sale by the Clearinghouse for Federal Scientific and Technical Information
Springfield, Virginia 22151 – CFSTI price $3.00

SUBSONIC LONGITUDINAL AERODYNAMIC MEASUREMENTS ON A TRANSPORT MODEL IN TWO SLOTTED TUNNELS DIFFERING IN SIZE

By Arvo A. Luoma, Richard J. Re,
and Donald L. Loving
Langley Research Center

SUMMARY

An investigation of the static longitudinal aerodynamic characteristics of the same 5-foot-span (1.5-meter) model of a large subsonic cargo-type transport was made in the Langley 8-foot transonic pressure tunnel and in the Langley 16-foot transonic tunnel at Mach numbers from 0.700 to 0.825. The Reynolds numbers, the test conditions, and the data-reduction procedures were the same in the two investigations.

The agreement in the data obtained was generally satisfactory. The greatest differences in the comparisons usually occurred at lift coefficients beyond the cruise lift where probably unequal effects of flow separation, particularly at supercritical speeds, may be expected. The results indicate that a model having a wing span which is large relative to the width of the test section can be tested in a slotted wind tunnel at subsonic speeds and that the results of such tests can be used with confidence provided the test techniques and data-reduction methods used adhere to acceptable standards developed for such tests.

INTRODUCTION

Since the advent of the first successful transonic wind tunnel in 1947 at the Langley Research Center (ref. 1), the preponderance of the research carried on in transonic tunnels has been directed toward a study of airplane and missile configurations intended to operate in and above the transonic-speed range. In recent years, however, increased interest and research have been directed toward the development of a new class of large military and commercial subsonic jet transports, and toward the improvement of the cruise efficiency of such airplanes at high subsonic speeds. As a result of this renewed interest in subsonic research, a substantial part of the research effort in the subsonic speed range is being carried out in transonic tunnels.

In wind-tunnel tests, a model as large as possible is generally desirable in order to obtain higher model Reynolds numbers. At transonic and supersonic speeds the model size is usually limited by the problem of boundary-reflected disturbances existing at Mach numbers greater than 1. This particular constraint on model size does not exist, of course, when the tests are to be made only at subsonic speeds. Since the wind tunnel with slotted walls has greatly reduced or eliminated the solid-blockage interference (ref. 1), a substantially larger model can be used for subsonic tests in a slotted wind tunnel than can be used for subsonic tests in a comparable closed-throat wind tunnel.

However, the slotted-tunnel configuration required to eliminate solid blockage cannot simultaneously satisfy the requirements needed to eliminate lift interference. (Specifically, the open ratio of the slotted walls required to eliminate solid blockage is greater than that required to eliminate lift interference; see ref. 2, for example.) Therefore, it is necessary to determine the magnitude of the downwash due to the tunnel-boundary interference on the lift of the model, particularly when the model is large relative to the width of the test section, in order to make any necessary corrections to the data. Theory shows that this lift interference is a function of the cross-sectional shape of the tunnel; the type, distribution, and amount of tunnel-wall ventilation; the ratio of wing span to tunnel width; the ratio of wing area to tunnel cross-sectional area; and the lift coefficient. A recent theoretical analysis of tunnel-boundary lift interference on wings in rectangular test sections with slotted top and bottom walls and solid side walls includes calculations of the spanwise variation of the interference and the effect of sweepback. (See ref. 3.) Application of the theory of reference 3 to a large sweptback model in the Langley 8-foot transonic pressure tunnel (which has a square test section with slotted top and bottom walls and solid side walls) indicates that the interference of the tunnel walls on the average induced flow is small, the spanwise variation of the interference from wing root to wing tip being approximately twice the average value.

Comparative static longitudinal aerodynamic data at Mach numbers from 0.700 to 0.825 were obtained on the same 5-foot-span (1.5-meter) model of a large subsonic cargo-type transport in the Langley 8-foot transonic pressure tunnel and in the Langley 16-foot transonic tunnel. Both of these tunnels are of the slotted type. The 5-foot-span (1.5-meter) model was much larger than usual for tests in the Langley 8-foot transonic pressure tunnel, the model wing span being two to three times that of the typical transonic models investigated in this tunnel. The main purpose of the two investigations was to establish experimentally the reliability of tests at subsonic speeds of a model having a wing span which was large relative to the width of the test section of the smaller slotted tunnel. The ratio of model wing span to tunnel width was 0.70 for the smaller tunnel and 0.32 for the larger tunnel. The Reynolds numbers in the two investigations were the same. The mean values of lift, drag, and pitching-moment results obtained from tests of the model upright and inverted with fixed boundary-layer transition on the model are

presented herein. The results for the upright configuration from the Langley 16-foot transonic tunnel investigation at Mach numbers from 0.50 to 0.85, as well as information on the effects of fixing transition, are presented in reference 4. A brief comparison of the drag data obtained in the two investigations is presented in reference 5.

SYMBOLS

The aerodynamic force and moment data are referred to the wind axes, with the origin located longitudinally at the fuselage station which contains the 25-percent point of the wing mean aerodynamic chord and vertically 3.80 centimeters (1.495 inches) above the fuselage reference line.

b	wing span
c	wing local chord
$\bar{c}$	wing mean aerodynamic chord
C_D	drag coefficient, $\frac{\text{Drag}}{qS}$
C_L	lift coefficient, $\frac{\text{Lift}}{qS}$
C_m	pitching-moment coefficient, $\frac{\text{Pitching moment}}{qS\bar{c}}$
M	free-stream Mach number
q	free-stream dynamic pressure
R	Reynolds number, based on a reference length of 0.3048 meter (1 foot)
S	wing area
α	angle of attack of model, based on fuselage reference line
δ_h	horizontal-tail deflection
$\frac{\Delta C_D'}{(\Delta C_L')^2}$	drag-due-to-lift factor

Subscript:

min minimum

Difference between Langley 8-foot transonic pressure tunnel (8-ft TPT) results and Langley 16-foot transonic tunnel (16-ft TT) results at the same value of C_L:

$$\Delta\alpha = (\alpha)_{8\text{-ft TPT}} - (\alpha)_{16\text{-ft TT}}$$

$$\Delta C_D = (C_D)_{8\text{-ft TPT}} - (C_D)_{16\text{-ft TT}}$$

$$\Delta C_m = (C_m)_{8\text{-ft TPT}} - (C_m)_{16\text{-ft TT}}$$

Increments referenced to values corresponding to minimum drag:

$$\Delta C'_D = C_D - C_{D,min}$$

$$\Delta C'_L = C_L - (C_L)_{at\ C_{D,min}}$$

APPARATUS

Tunnels

The investigations were made in the Langley 8-foot transonic pressure tunnel and in the Langley 16-foot transonic tunnel. The Langley 8-foot transonic pressure tunnel is a single-return pressure wind tunnel with a test section 7.1- by 7.1-foot square (equivalent in area to an 8.0-foot-diameter (2.44-meter) circle) and having solid side walls and axially slotted top and bottom walls. The test-section Mach number can be continuously varied from 0 to 1.3. The total pressure of the tunnel air can be varied from a minimum value of about 0.1 atmosphere at all test Mach numbers to a maximum value of about 1.5 atmospheres at transonic Mach numbers and about 2.0 atmospheres at Mach numbers of 0.4 or less. (1 atmosphere = 1×10^5 newtons/meter^2.) The stagnation temperature of the tunnel air is automatically controlled and is usually held constant at 120° F (322° K). The tunnel air is dried until the dewpoint temperature in the test section is reduced sufficiently to avoid condensation effects.

The Langley 16-foot transonic tunnel is a single-return atmospheric wind tunnel with an octagonal test section 15.5 feet between walls (equivalent in area to a 16.0-foot-diameter (4.88-meter) circle) and having axial slots at the wall vertices. A more detailed description of this tunnel is given in reference 6.

Model

The same 0.023-scale model of a large subsonic cargo-type transport was investigated in both the Langley 8-foot transonic pressure tunnel and the Langley 16-foot transonic tunnel. A three-view drawing of the complete model configuration tested is shown in figure 1, and details of model components are shown in figures 2 to 5.

Wing.- The wing had the planform geometry shown in figure 2, and the wing airfoil sections (streamwise) were NACA four-digit series with mean camber lines for design lift coefficients of 0.266 at the 20-percent semispan station, 0.321 at the 43-percent semispan station, and 0.336 at the 70-percent semispan station. The wing thickness ratio varied along the span and was 12.4 percent at the 20-percent semispan station, 11.1 percent at the 43-percent semispan station, and 11.0 percent at the 70-percent semispan station. The wing had 3.5° of twist, was mounted at an angle of incidence of 3.5° at the wing root, and had a dihedral angle of -3.5°.

Nacelle-pylon configuration.- The geometry of the four pylon-mounted nacelles included on the model in the comparison studies is shown in figure 3. The external surface of the nacelles was contoured to an NACA 1-series section at the forward portion and to a circular-arc section at the rear portion. The nacelle internal lines were cylindrical (4.32 cm in diameter) to a nacelle station just forward of the duct exit. The airfoil section of the pylons was NACA 66-008 streamwise.

Horizontal and vertical tails.- Figures 4 and 5 show the geometry of the horizontal and vertical tails, respectively. The horizontal and vertical tails had modified NACA four-digit series airfoil sections streamwise and were 10.5- and 13-percent thick, respectively. The horizontal tail was set at a deflection angle of 0° for these tests.

Model installation.- The method of installation of the sting-mounted model in the Langley 8-foot transonic pressure tunnel is indicated in figure 6. Photographs of the sting-mounted model installed in the Langley 8-foot transonic pressure tunnel and in the Langley 16-foot transonic tunnel are shown as figures 7 and 8, respectively. The model was supported in both tunnels by the same model sting, which had a cross section 5.72 cm in width and 8.90 cm in depth (2.25 in. by 3.50 in.) with flat sides and rounded top and bottom. (See figs. 7(b) and 8(b).) The distance from the balance center to the end of the model sting was 168.3 cm (66.30 in.). The model sting was attached to the remotely operated tunnel central support systems.

The ratio of model wing span to tunnel width, the ratio of model wing area to tunnel cross-sectional area, and the model blockage were 0.70, 0.0632, and 1.7 percent, respectively, for the investigation in the Langley 8-foot transonic pressure tunnel and 0.32, 0.0158, and 0.4 percent, respectively, for that in the Langley 16-foot transonic tunnel.

Instrumentation

Aerodynamic forces and moments were measured in both investigations with the same six-component internal strain-gage balance housed in the model body. The model angle of attack was measured with a strain-gage attitude indicator located in the model nose. Static pressures within the balance chamber and the fuselage-sting cavity were measured with differential pressure transducers.

TESTS, CORRECTIONS, AND ACCURACY

As mentioned previously, the model and the model sting used in the investigations in the two tunnels were the same. Also, the same model configuration in both the upright and the inverted positions was tested with fixed boundary-layer transition on the model in each tunnel. The inverted position of the model was obtained by rotating the model, the balance, and the model sting as an integral unit 180° from the upright position. The test Mach numbers, the test Reynolds numbers, and the transition grit size and location on the model components were the same in the two investigations.

Comparisons of the longitudinal aerodynamic data were obtained at Mach numbers from 0.700 to 0.825 and at angles of attack from approximately -4° to 6°. The cruise specifications for the transport investigated included a Mach number of approximately 0.775 and a lift coefficient of approximately 0.5. The test Reynolds numbers based on a reference length of 0.3048 meter (1 foot) varied from 3.3×10^6 to 3.6×10^6 over the Mach number range.

Transition strips of carborundum particles were placed on both surfaces of the wing, the horizontal and vertical tails, and the pylons at 10 percent of the local chord (streamwise). Transition strips were also located on the nacelles (outside and inside) at 10 percent of the nacelle length, on the wheel-well fairings at 10 percent of the fairing length, and on the fuselage nose 5.08 centimeters from the tip of the nose. The width of the transition strips was 0.25 centimeter. Number 100 grit was used on all model components except the horizontal tail, where number 120 grit was used. The effect on the aerodynamic characteristics of fixing transition was also determined in the investigation in the Langley 16-foot transonic tunnel; this effect was found to be substantial. (See ref. 4.)

The angle of attack has been corrected for the tunnel airflow angularity as determined by the tests of the model upright and the model inverted. A theoretical tunnel-wall lift interference correction has been made to the data; this correction consisted of reducing the angle of attack by $0.10C_L$ degree for the data obtained in the Langley 8-foot transonic pressure tunnel and by $0.02C_L$ degree for the data obtained in the Langley 16-foot transonic tunnel. The main significance of this angle correction shows up as a

reduction in drag coefficient, amounting at a lift coefficient of 0.5, for example, to about 0.0005 for the 8-foot transonic pressure tunnel drag values and about 0.0001 for the 16-foot transonic tunnel drag values. The lift, drag, and pitching-moment coefficients have been corrected for the balance chamber and sting-fuselage cavity pressures. The base drag correction reduced the drag coefficient generally by 0.0001 or 0.0002 in the 8-foot transonic pressure tunnel tests and by 0.0005 or 0.0006 in the 16-foot transonic tunnel. The drag coefficient also has been corrected for the calculated internal drag coefficient of the four nacelles; this correction amounted to 0.0007 at all Mach numbers. The drag coefficient has been further corrected for buoyancy; this correction increased the drag coefficient by 0.0003 in the 8-foot transonic pressure tunnel tests and by 0.0002 or 0.0003 in the 16-foot transonic tunnel tests.

The lift, drag, and pitching-moment coefficients have also been corrected for model-upright—model-inverted differences, by adjusting the uncorrected coefficients at a given value of angle of attack by half the difference between the faired values for the model upright and the corresponding faired values for the model inverted. The resulting corrected values are therefore the mean values of the model-upright and model-inverted values.

No corrections were made to the data for sting interference. Since the sting corrections should be the same in the two investigations, the corrections would have no effect on the comparison of the data. Anyway, the results of reference 7 showed that the sting interference was small.

The accuracy of the data, based primarily on the static calibrations of the instrumentation, on the repeatability of the test data, and on a probable improvement in reliability due to the averaging of the results for the upright and inverted configurations, is estimated to be as follows:

M	± 0.005
α, deg	± 0.05
C_L	± 0.007
C_D	± 0.0005
C_m	± 0.003

PRESENTATION OF RESULTS

A comparison of the basic longitudinal aerodynamic characteristics as obtained from the investigations in the Langley 8-foot transonic pressure tunnel and in the Langley 16-foot transonic tunnel is presented in figures 9 to 11. Two test-point symbols are used in the plots shown herein to represent the data from each tunnel – the first symbol for each tunnel indicating the corrected data from the tests of the upright configuration and

the second symbol, the corrected data from the tests of the inverted configuration. As pointed out in the section "Tests, Corrections, and Accuracy," the test-point values have been adjusted for the difference between the data for the upright configuration and the data for the inverted configuration. The results shown are therefore the mean values from tests of the model upright and the model inverted.

The variation with lift coefficient of the difference between the Langley 8-foot transonic pressure tunnel results and the Langley 16-foot transonic tunnel results is shown in figure 12. This difference was obtained from figures 9 to 11. It should be noted that the angle-of-attack and drag scales used in figure 12 have been expanded compared with the corresponding scales used in figures 9 and 10. Drag-due-to-lift information is given in figures 13 and 14.

DISCUSSION

Tunnel-Boundary Lift Interference in Transonic Tunnels

Other investigations.- Comparisons of aerodynamic measurements from different wind tunnels on the same or on an equivalent model have at times proved to be a somewhat touchy subject. However, unsatisfactory correlation in measurements usually can be reconciled when proper consideration is given to differences in models, test conditions, test techniques, flow angularity, tunnel-wall effects, data corrections, and so forth. (See ref. 5.) Several cases of unsatisfactory correlation in aerodynamic measurements (unpublished) have been noted in tests in transonic tunnels at subsonic speeds on relatively large models. Most of this lack of correlation was traced to a failure to correct the results for tunnel-wall lift interference. When the results from slotted-tunnel tests were corrected for theoretical lift interference, by available methods such as those of reference 2, the correlation became good. Other tests of a model in a tunnel which was operated first in the slotted configuration and then in the closed configuration gave results which were in good agreement after theoretical corrections had been made to the data for wall effects. Comparative results were also obtained from perforated-tunnel tests. However, theoretical methods were not available at the time of the tests for correcting these results for lift interference. The uncorrected angles of attack and drags from the tests in the perforated tunnel were higher at lifting conditions than the corresponding theoretically corrected values from the tests in the slotted and closed tunnels. In other words, the lift interference of the perforated boundary was approaching that of an open boundary.

The tunnel-boundary lift interference of perforated test sections is less amenable to theoretical treatment than that of slotted test sections, and the practical application of such theory presents further problems because of the difficulty in the estimation of an effective permeability constant. A recent theoretical study of the tunnel-boundary lift

interference on wings in rectangular perforated test sections is presented in reference 8. The analysis in this reference also considers the spanwise variation of the interference.

Present investigations.- In the comparison investigations reported herein, the same 5-foot-span (1.5-meter) model of a large subsonic cargo-type transport was tested at subsonic speeds in two slotted tunnels differing substantially in size. The ratio of model wing span to tunnel width, the ratio of model wing area to tunnel cross-sectional area, and the model blockage were 0.70, 0.0632, and 1.7 percent, respectively, for the investigation in the smaller tunnel and 0.32, 0.0158, and 0.4 percent, respectively, for that in the larger tunnel. The wing span of the model relative to the width of the test section of the smaller tunnel is considered to be large.

The smaller tunnel has a square test section with slotted top and bottom walls and solid side walls. The theoretical effect of this particular slotted tunnel configuration on a lifting wing is to produce an interference downflow at the midspan of the wing and a relative upflow (relative, that is, to the interference flow at the midspan section) which increases toward the wing tip. (See ref. 3.) At a lift coefficient of 0.5, for example, the theoretical spanwise variation of the relative upflow from wing root to wing tip amounted to 0.11° for the model investigated. A spanwise variation of interference flow is certainly undesirable; however, the magnitude of this spanwise variation in the present tests was small, and the spanwise variation did have the effect of reducing the magnitude of the average induced flow to the model (compared with the interference flow at the midspan section). The theoretical average induced flow to the model at the lift coefficient of 0.5, for example, was a downflow of only 0.05°. A reduction in angle of attack by this amount results in a reduction in drag coefficient of 0.0005 at the lift coefficient of 0.5.

The lift interference on the model in the larger tunnel was much less as one might expect. The theoretical average induced flow to the model at the lift coefficient of 0.5 was a downflow of 0.01°. The change in drag coefficient corresponding to this change in angle of attack was a reduction of 0.0001.

Comparison of Aerodynamic Results From Present Investigations

The minimum drags obtained in the investigations in the two slotted tunnels were the same within 1 or 2 counts of drag (where 1 count of drag is equivalent to a drag coefficient of 0.0001) at all Mach numbers except 0.825; at this Mach number, the difference was 6 counts of drag, which is still small in relation to the accuracy of the data. (See fig. 10.) At lifting conditions up to the cruise lift coefficient of approximately 0.5, the drag data differed by varying amounts from 0 to 10 counts of drag, depending on Mach number and lift coefficient. At the approximate cruise conditions of Mach number 0.775 and lift coefficient 0.5, the deviation in the drag data was no greater than about 4 counts

of drag, or 1 percent (fig. 10(c)). At high lift coefficients, where the drag is increasing rapidly with lift, the differences in the drag data were generally greater than at the lower lift coefficients.

The differences in drag data noted in figure 10 were generally a reflection of the angle-of-attack differences shown by the results in figure 9; that is, if at a given lift coefficient the angle of attack was higher for one set of data, then the corresponding drag would also be higher for this set of data. This effect of a difference in angle of attack on drag coefficient at a given value of lift coefficient is given by the equation

$$\Delta C_D = (C_L)(\Delta\alpha_{rad})$$

where ΔC_D is the resulting change in drag coefficient and $\Delta\alpha_{rad}$ is the difference in angle of attack expressed in radians.

The pitching-moment results presented in figure 11 generally agreed within the accuracy of the data. The largest differences between the pitching-moment data, as was also true of angle of attack (fig. 9) and drag (fig. 10), usually occurred at the highest lift coefficients, where probably unequal effects of flow separation, particularly at supercritical speeds, may be expected.

The variation with Mach number of the drag-due-to-lift factor is shown in figure 14. This variation with Mach number is seen to be essentially the same for the two sets of data, the magnitudes being generally somewhat lower for the data from the larger tunnel. The drag-due-to-lift factor shown is for the linear-variation range of the data of figure 13; this linear-variation range extended up to a lift coefficient of about 0.5 for Mach numbers of 0.775 and less.

CONCLUDING REMARKS

The agreement in the data obtained on the same 5-foot-span (1.5-meter) model of a large subsonic cargo-type transport from investigations at subsonic speeds in the Langley 8-foot transonic pressure tunnel and in the Langley 16-foot transonic tunnel was generally satisfactory. The greatest differences in the comparisons usually occurred at lift coefficients beyond the cruise lift where probably unequal effects of flow separation, particularly at supercritical speeds, may be expected.

The experimental comparative results indicate that a model having a wing span which is large relative to the width of the test section can be tested in a slotted wind

tunnel at subsonic speeds and that the results of such tests can be used with confidence provided the test techniques and data-reduction methods used adhere to acceptable standards developed for such tests.

Langley Research Center,
National Aeronautics and Space Administration,
Langley Station, Hampton, Va., May 20, 1968,
737-01-00-04-23.

REFERENCES

1. Wright, Ray H.; and Ward, Vernon G.: NACA Transonic Wind-Tunnel Test Sections. NACA Rep. 1231, 1955. (Supersedes NACA RM L8J06.)

2. Davis, Don D., Jr.; and Moore, Dewey: Analytical Study of Blockage- and Lift-Interference Corrections for Slotted Tunnels Obtained By the Substitution of an Equivalent Homogeneous Boundary for the Discrete Slots. NACA RM L53E07b, 1953.

3. Wright, Ray H.; and Barger, Raymond L.: Wind-Tunnel Lift Interference on Sweptback Wings in Rectangular Test Sections With Slotted Top and Bottom Walls. NASA TR R-241, 1966.

4. Re, Richard J.: Longitudinal Aerodynamic Characteristics of a Model of a Large Subsonic Jet Transport at Mach Numbers From 0.50 to 0.85. NASA TM X-1406, 1967.

5. Bielat, Ralph P.; Luoma, Arvo A.; and Daugherty, James C.: Drag Measurements From Different Wind Tunnels. NASA TM X-1271, 1966.

6. Ward, Vernon G.; Whitcomb, Charles F.; and Pearson, Merwin D.: Air-Flow and Power Characteristics of the Langley 16-Foot Transonic Tunnel With Slotted Test Section. NACA RM L52E01, 1952.

7. Loving, Donald L.; and Luoma, Arvo A.: Sting-Support Interference on Longitudinal Aerodynamic Characteristics of Cargo-Type Airplane Models at Mach 0.70 to 0.84. NASA TN D-4021, 1967.

8. Wright, Ray H.; and Schilling, Benferd L: Approximation of the Spanwise Distribution of Wind-Tunnel-Boundary Interference on Lift of Wings in Rectangular Perforated-Wall Test Sections. NASA TR R-285, 1968.

Wing	
Aspect ratio	7.75
Area, m^2	0.2949
Mean aerodynamic chord, cm	21.33
Span, m	1.512
Horizontal stabilizer	
Aspect ratio	5.21
Taper ratio	0.37
Area, m^2	0.0418
Mean aerodynamic chord, cm	9.59
Span, m	0.467
Vertical stabilizer	
Aspect ratio	1.24
Taper ratio	0.61
Area, m^2	0.0308
Mean aerodynamic chord, cm	16.35
Span, m	0.199

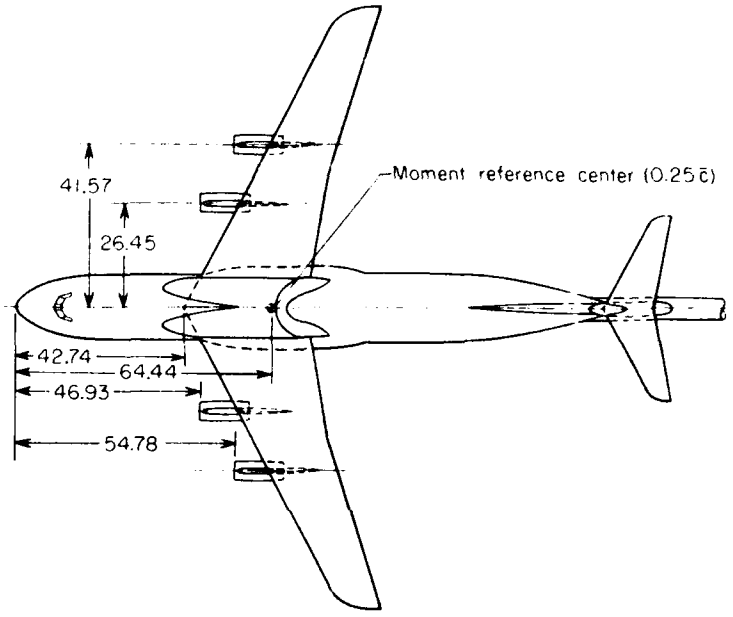

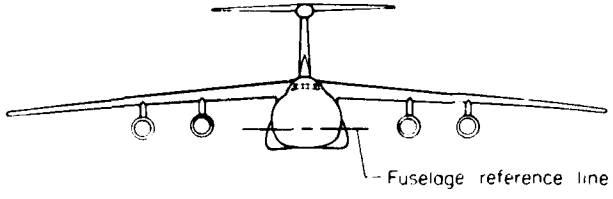

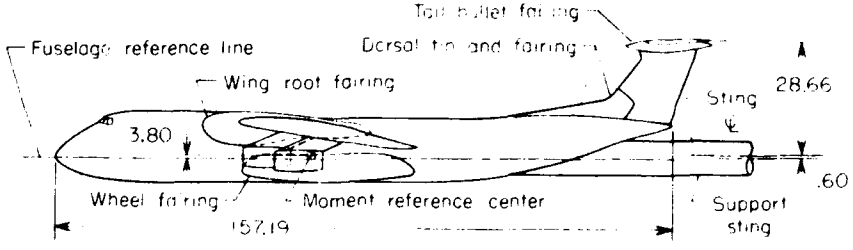

Figure 1.- Three-view drawing of 0.023-scale model of large subsonic cargo-type transport. All dimensions are in centimeters unless otherwise noted.

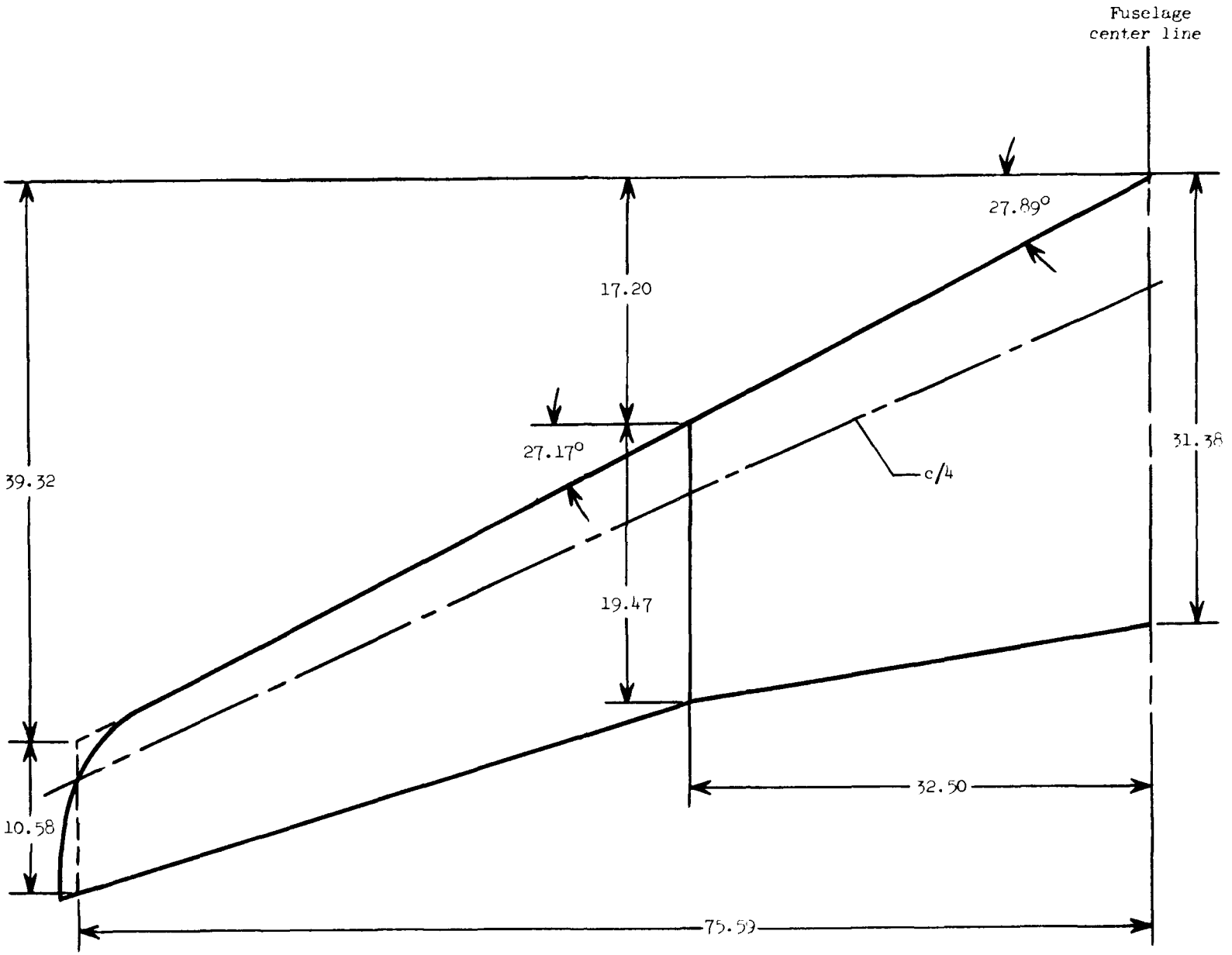

Figure 2.- Geometry of projected wing planform. All dimensions are in centimeters unless otherwise noted.

Dimension	Inboard nacelle	Outboard nacelle
C	10.12	10.07
D	5.74	5.60
E	.63	.45
F	.32	.25
G	.30	.23
H	1.66	.35

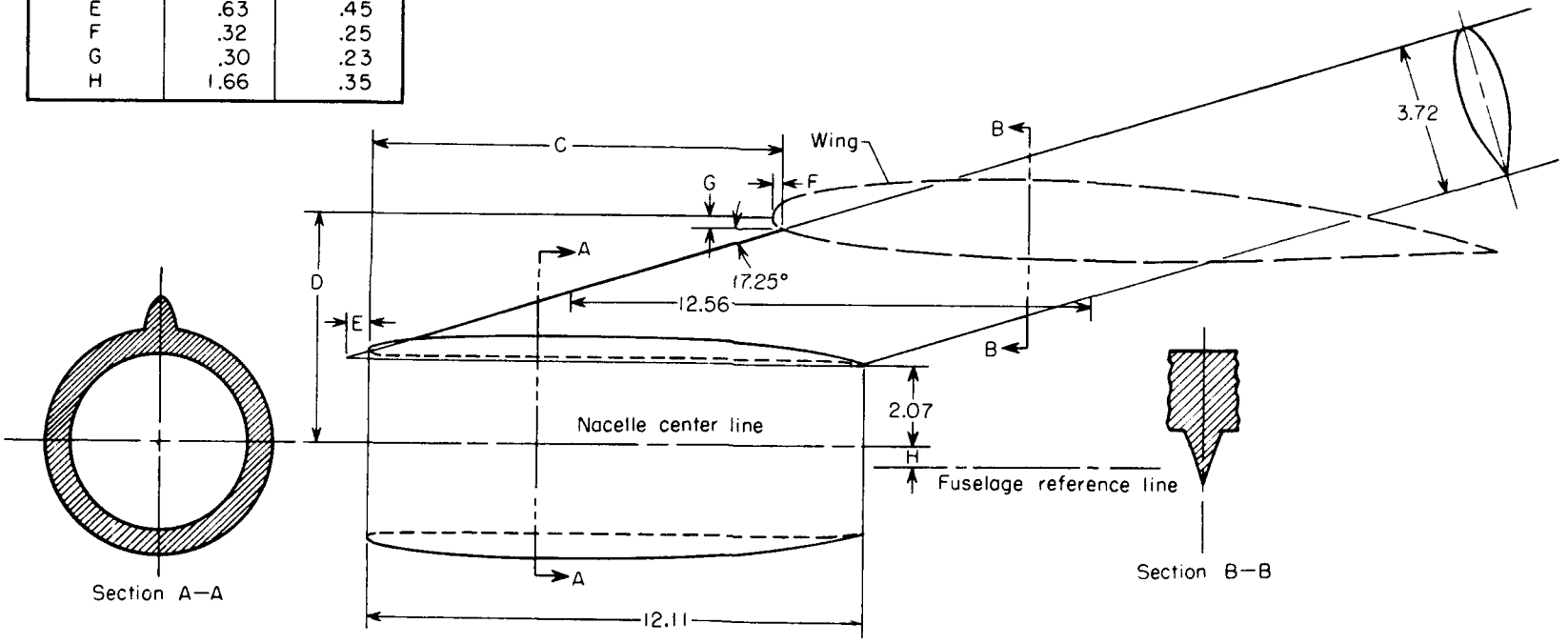

Figure 3.- Geometry of pylon-nacelle configuration included on model in comparison studies. All dimensions are in centimeters unless otherwise noted.

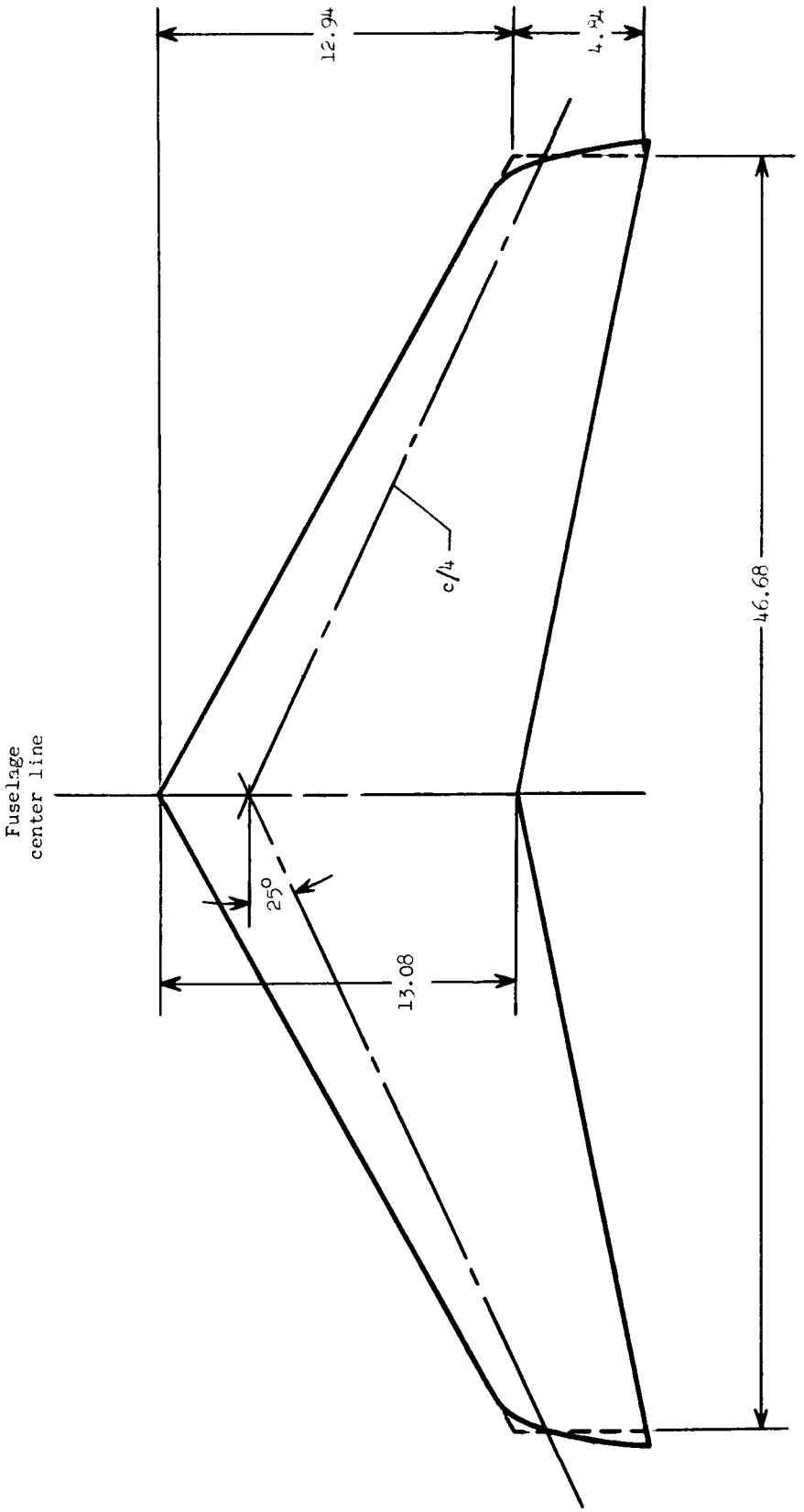

Figure 4.- Geometry of horizontal tail. All dimensions are in centimeters unless otherwise noted.

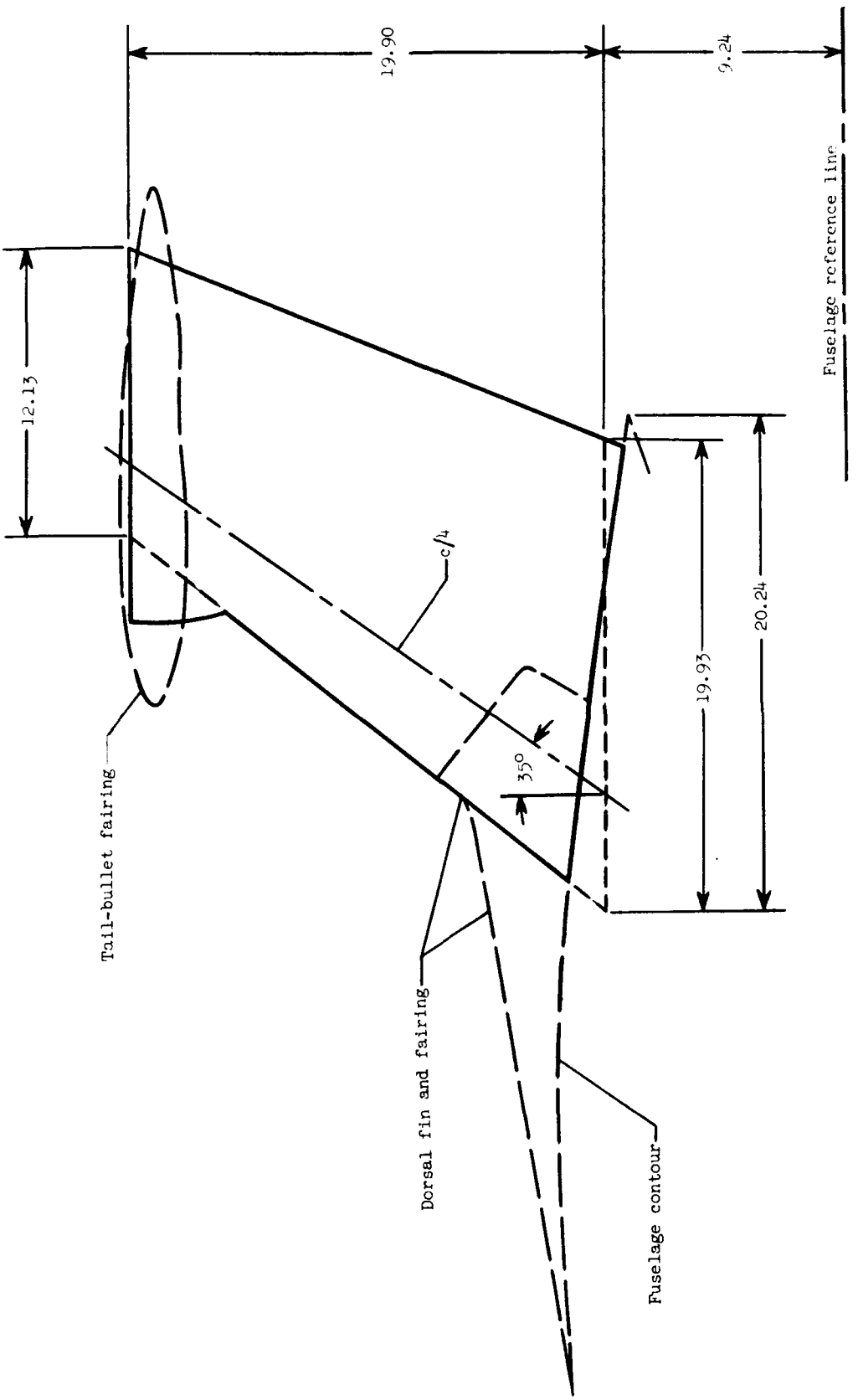

Figure 5.- Geometry of vertical tail. All dimensions are in centimeters unless otherwise noted.

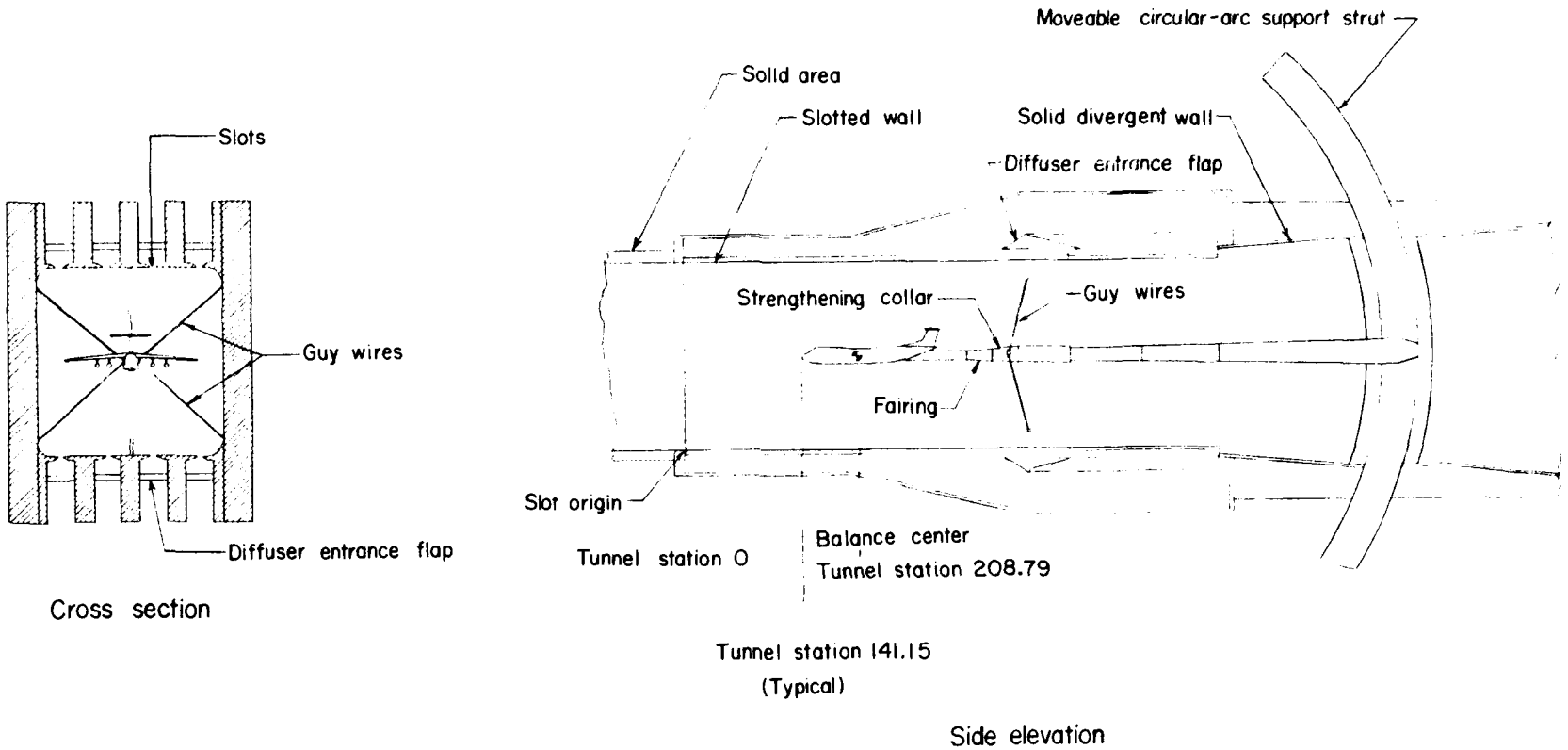

Figure 6.- Method of installation of 0.023-scale model of large subsonic cargo-type transport for sting-mounted tests in the Langley 8-foot transonic pressure tunnel. All dimensions are in centimeters.

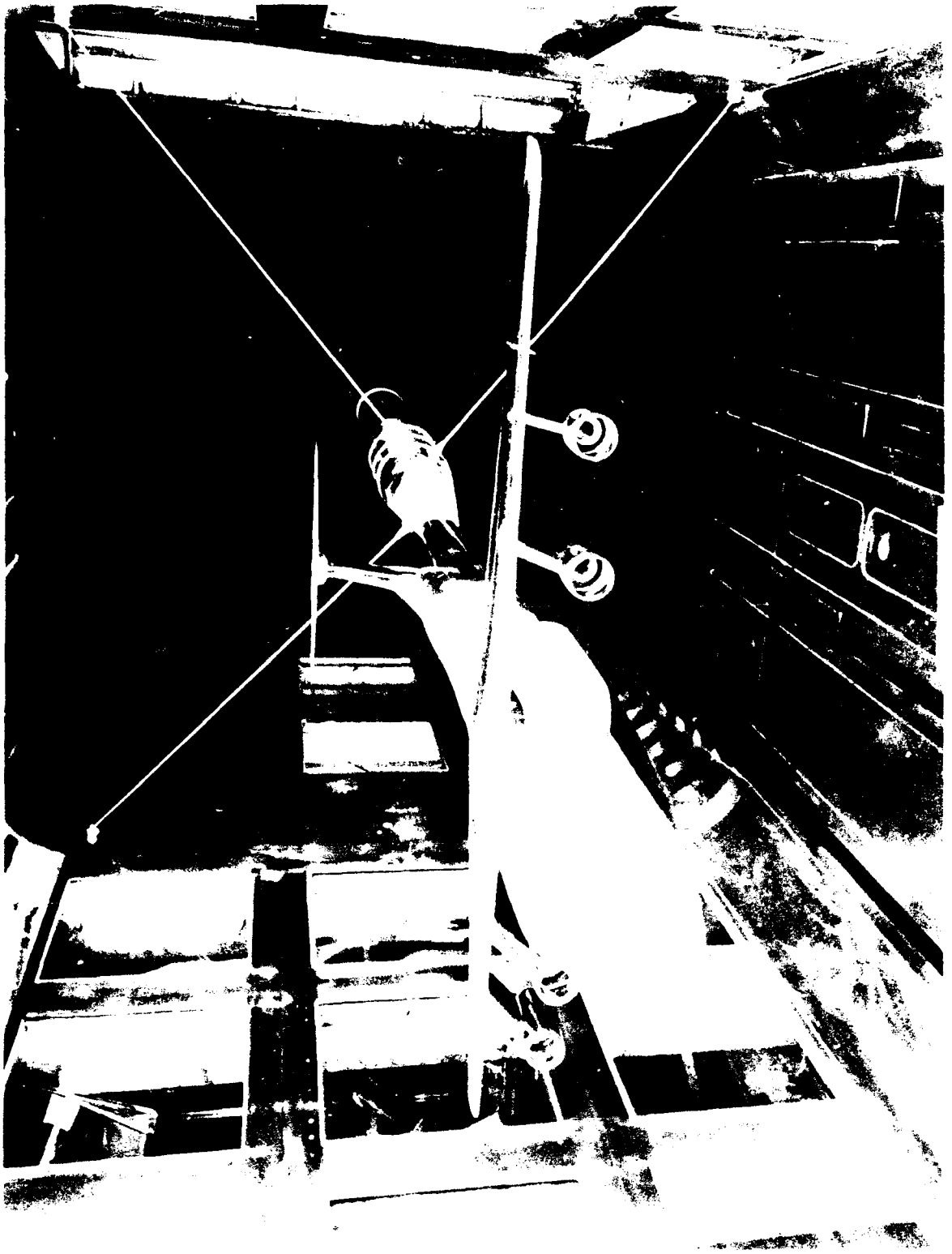

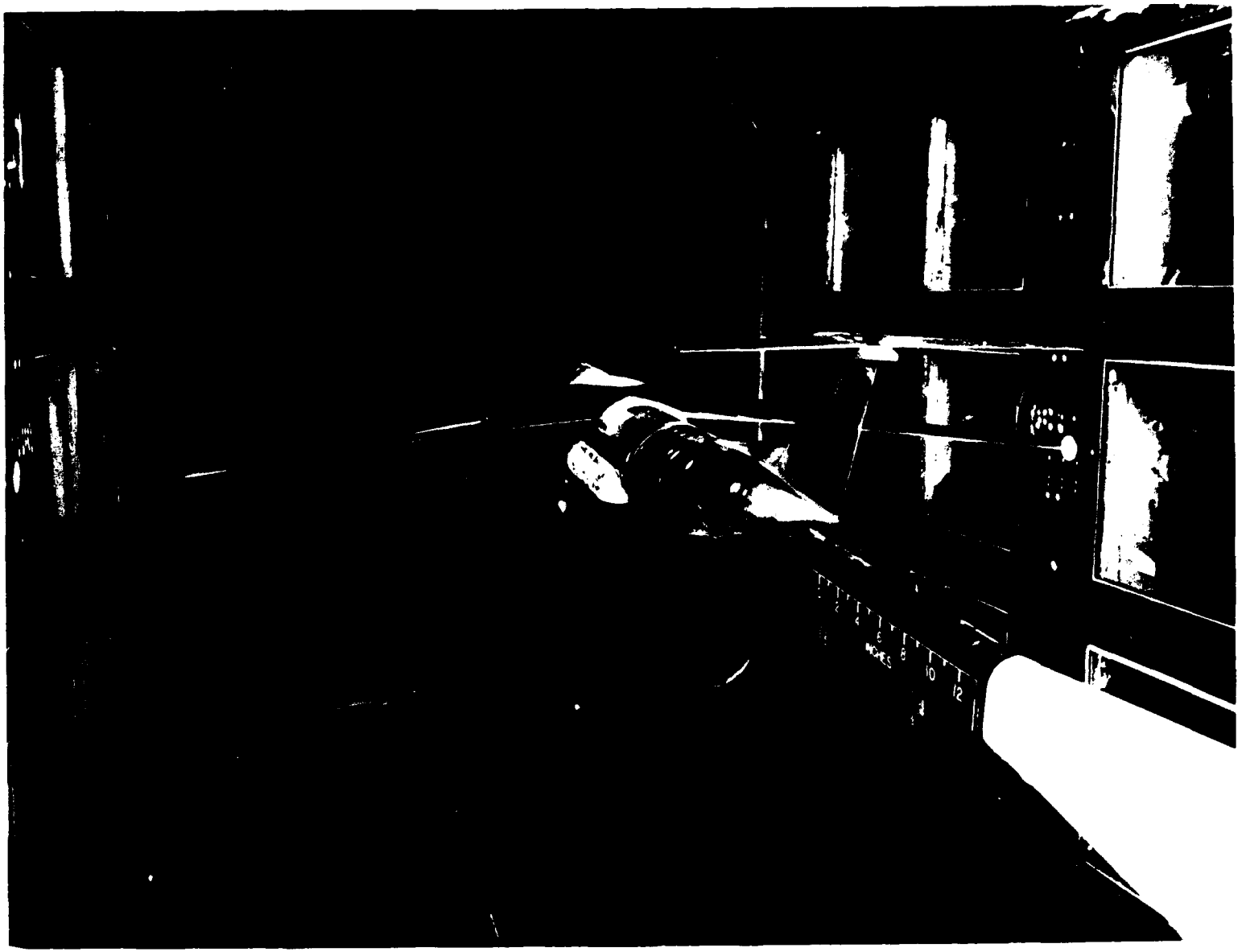

(b) Three-quarter rear view. L-65-1896

Figure 7.- Concluded.

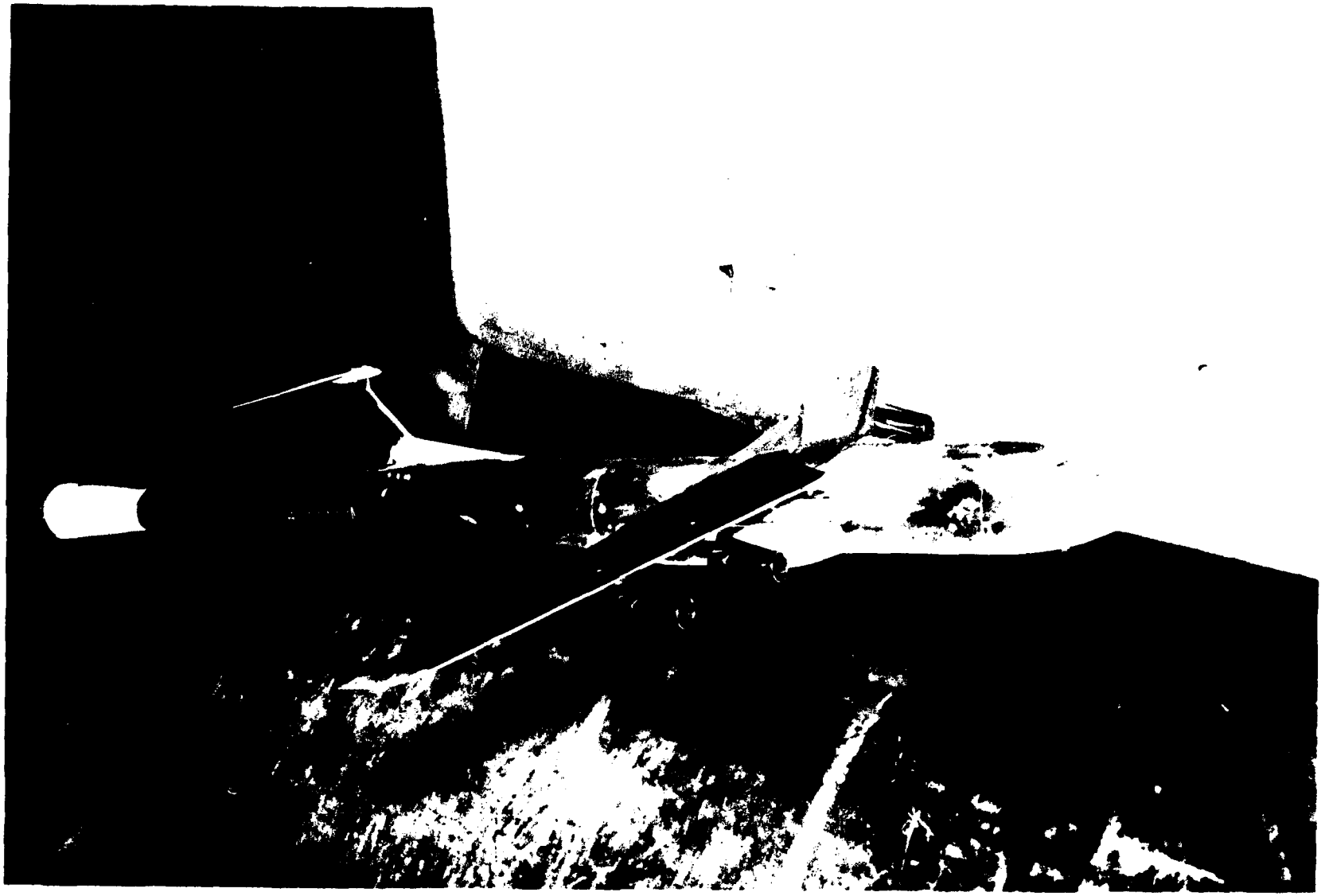

Figure 8.– Photographs of 0.02-scale model of large [illegible] transport airplane showing [illegible] in the Langley 16-foot transonic tunnel, R_c = [illegible]. The pylon nacelle configuration shown was [illegible] comparison studies.

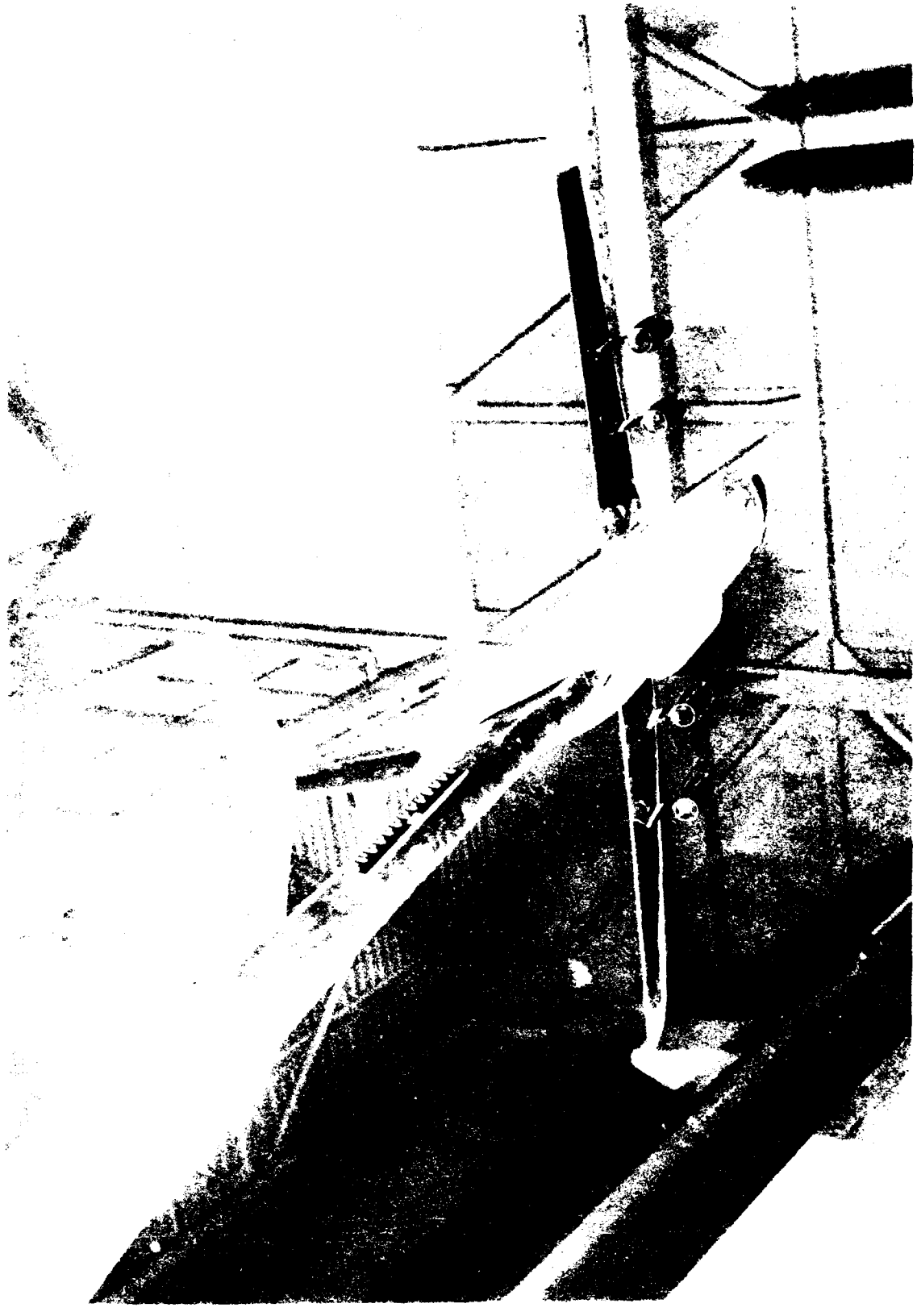

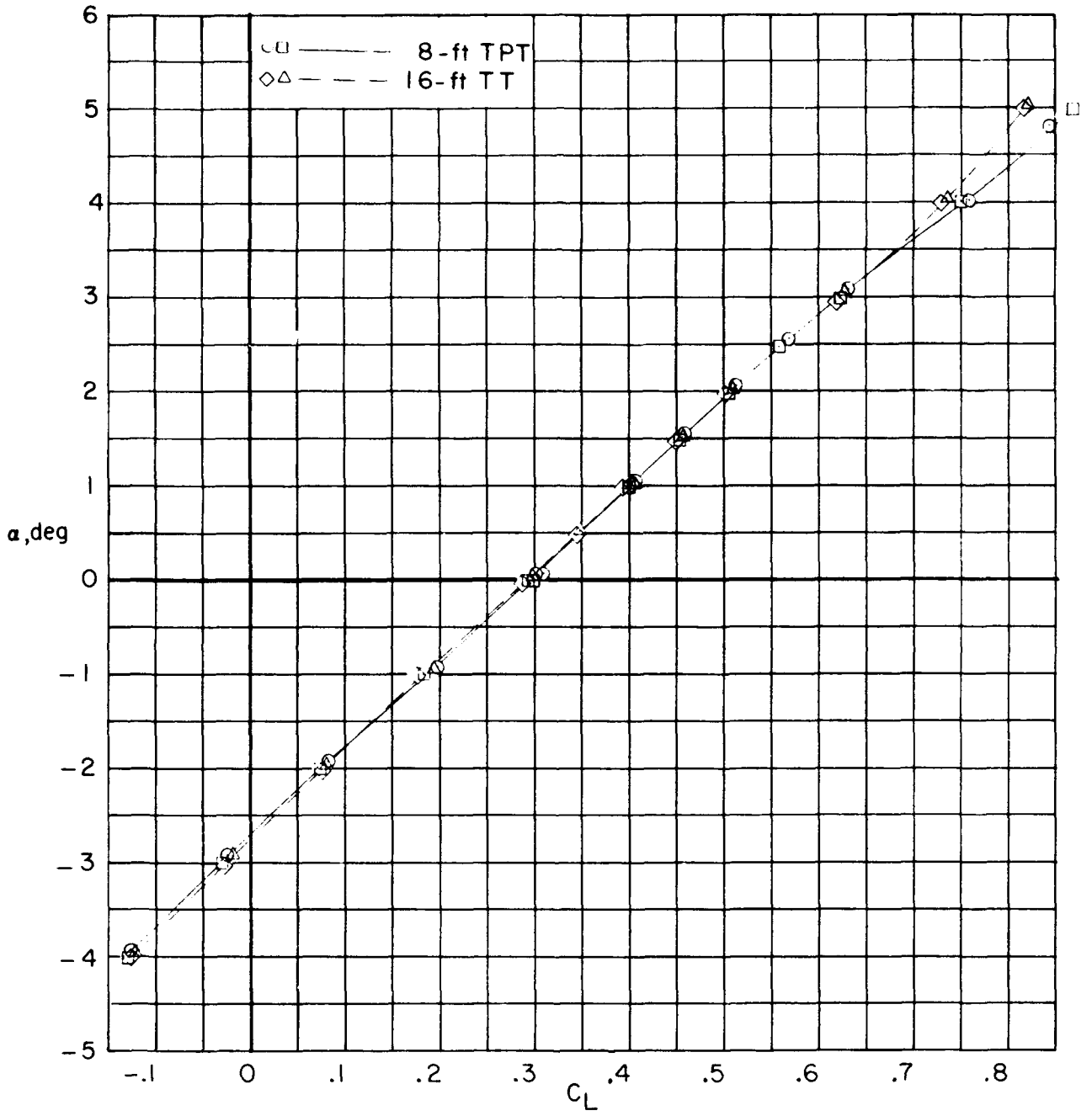

(a) M = 0.700; R = 3.3 × 10^6.

Figure 9.- Comparison of plots of angle of attack against lift coefficient for a large subsonic cargo-type transport from tests in the Langley 8-foot transonic pressure tunnel (8-ft TPT) and in the Langley 16-foot transonic tunnel (16-ft TT). $\delta_h = 0^0$.

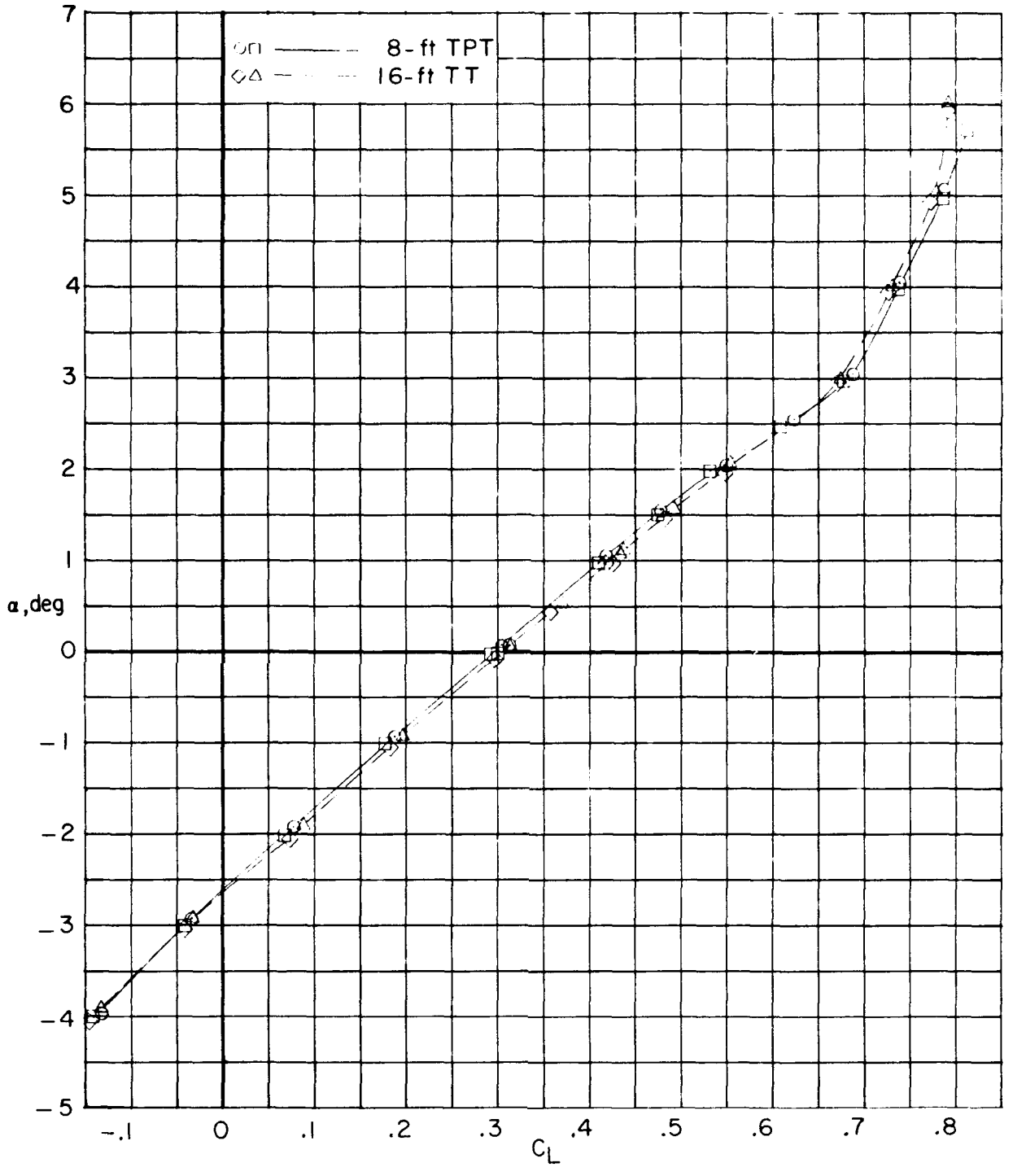

(b) M = 0.750; R = 3.4 × 10^6.

Figure 9.- Continued.

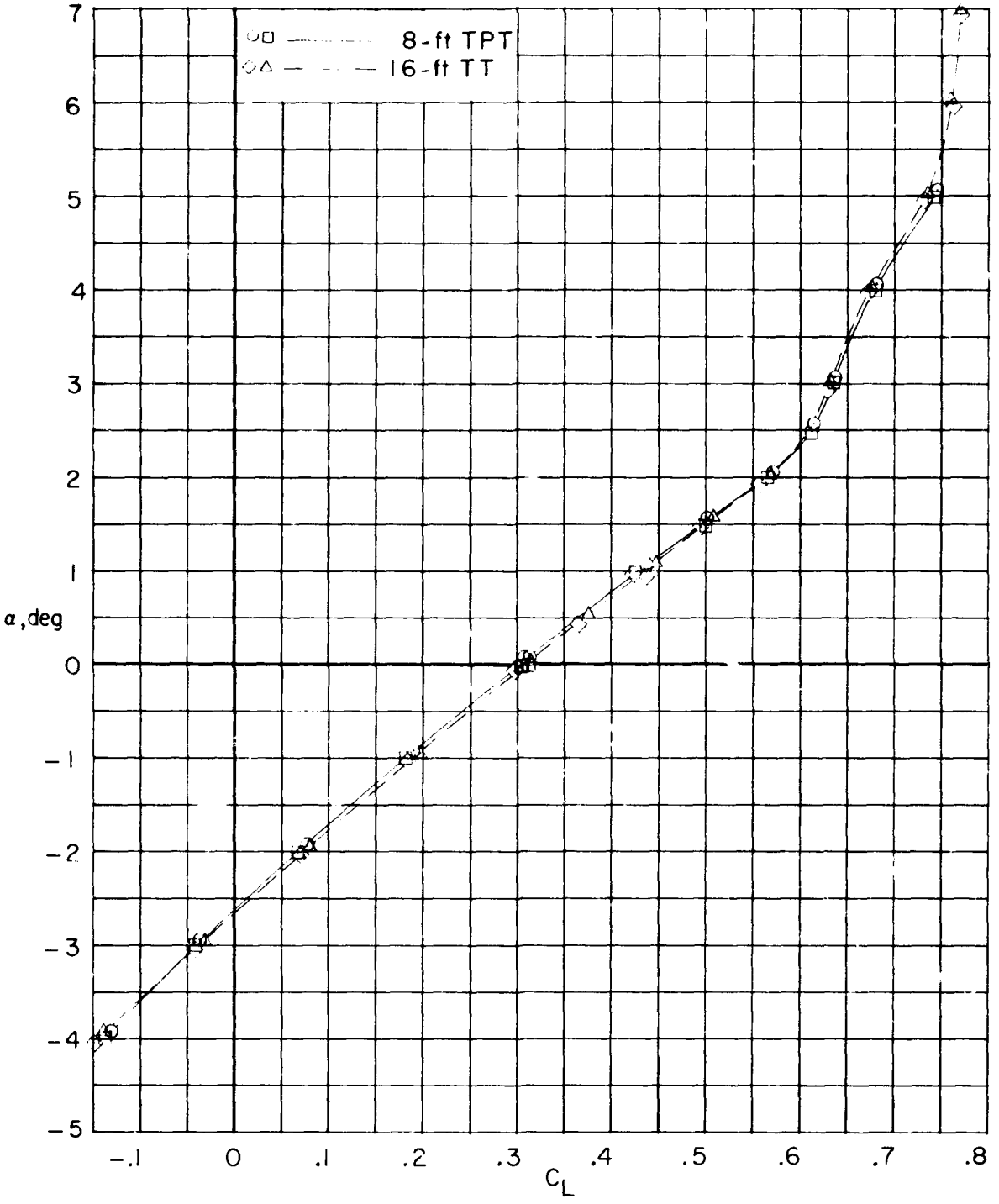

(c) M = 0.775; R = 3.5 × 10^6.

Figure 9.- Continued.

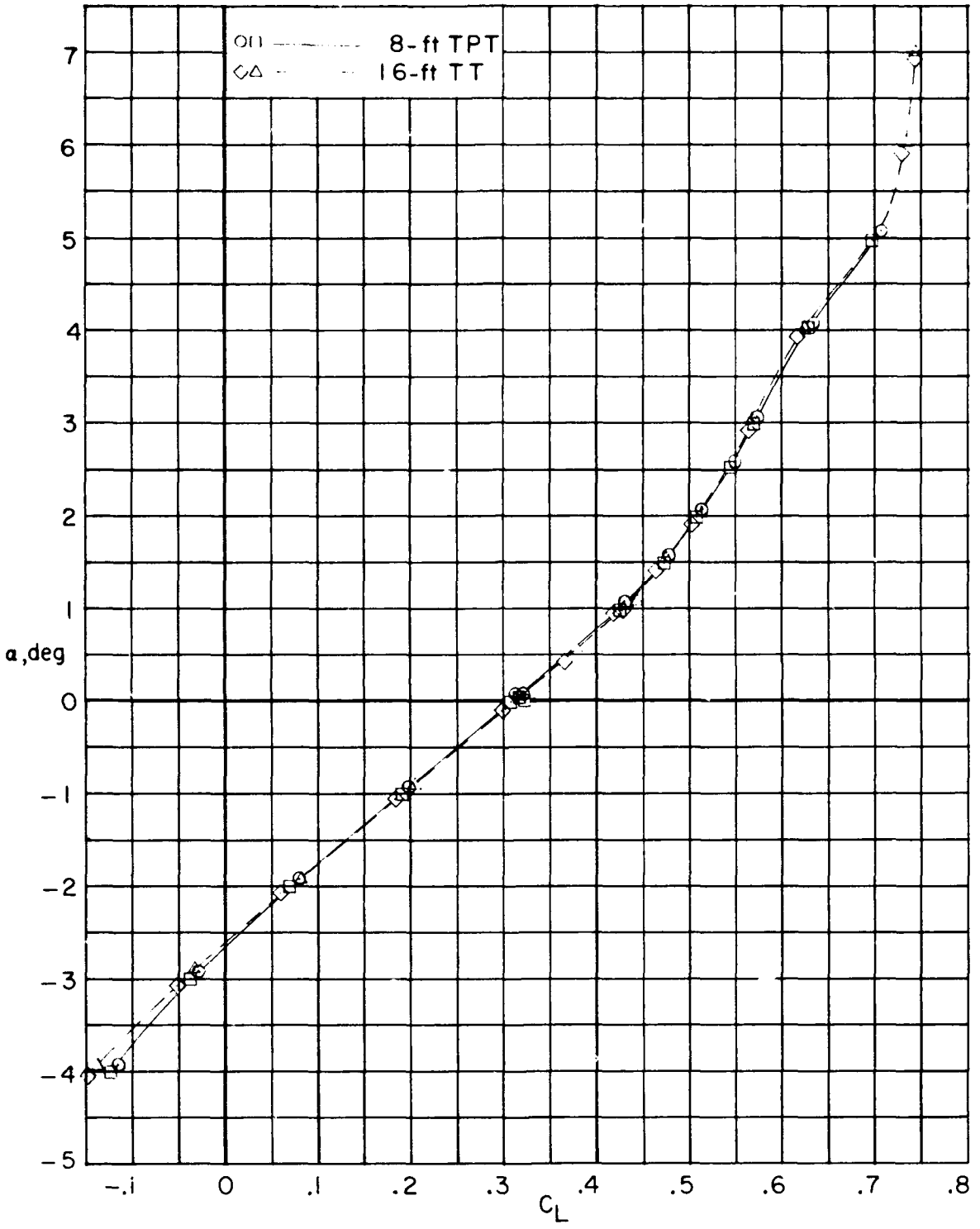

(d) M = 0.800; R = 3.5 × 10^6.

Figure 9.- Continued.

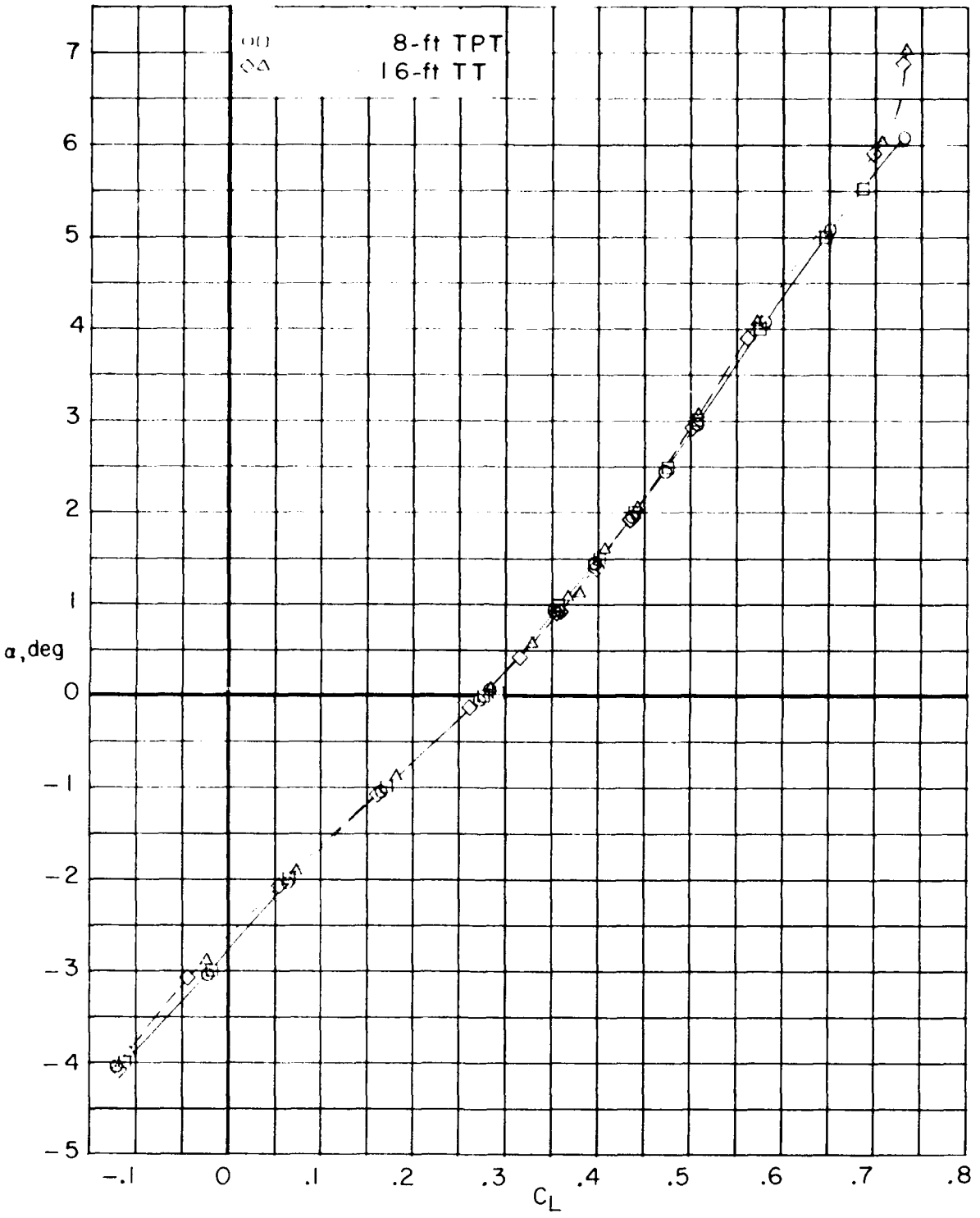

(e) M = 0.825; R = 3.6 × 10^6.

Figure 9.- Concluded.

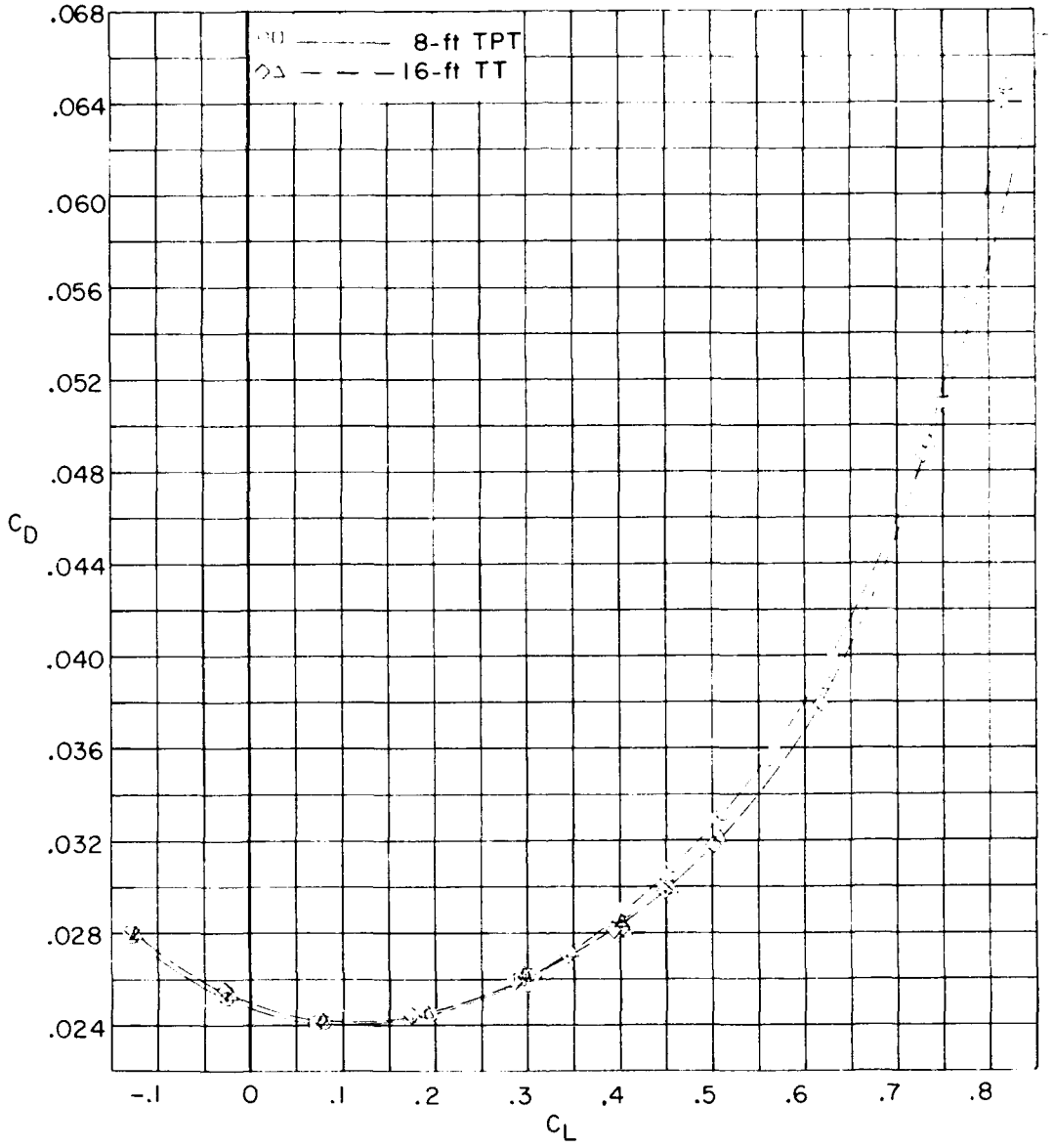

(a) M = 0.700; R = 3.3 × 10^6.

Figure 10.- Comparison of lift-drag polars for a large subsonic cargo-type transport from tests in the Langley 8-foot transonic pressure tunnel (8-ft TPT) and in the Langley 16-foot transonic tunnel (16-ft TT). $\delta_h = 0^o$.

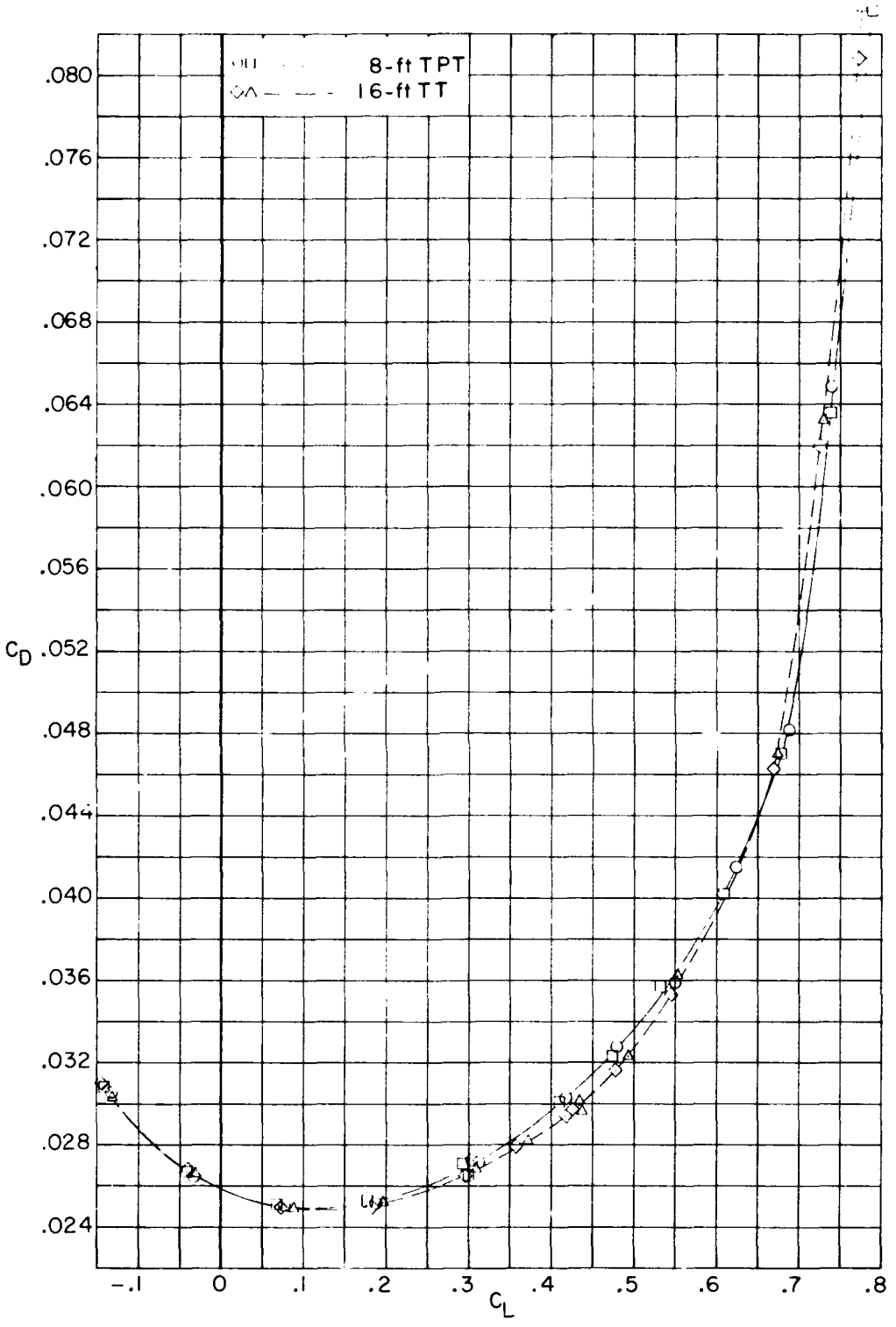

(b) M = 0.750; R = 3.4 × 10^6.

Figure 10.- Continued.

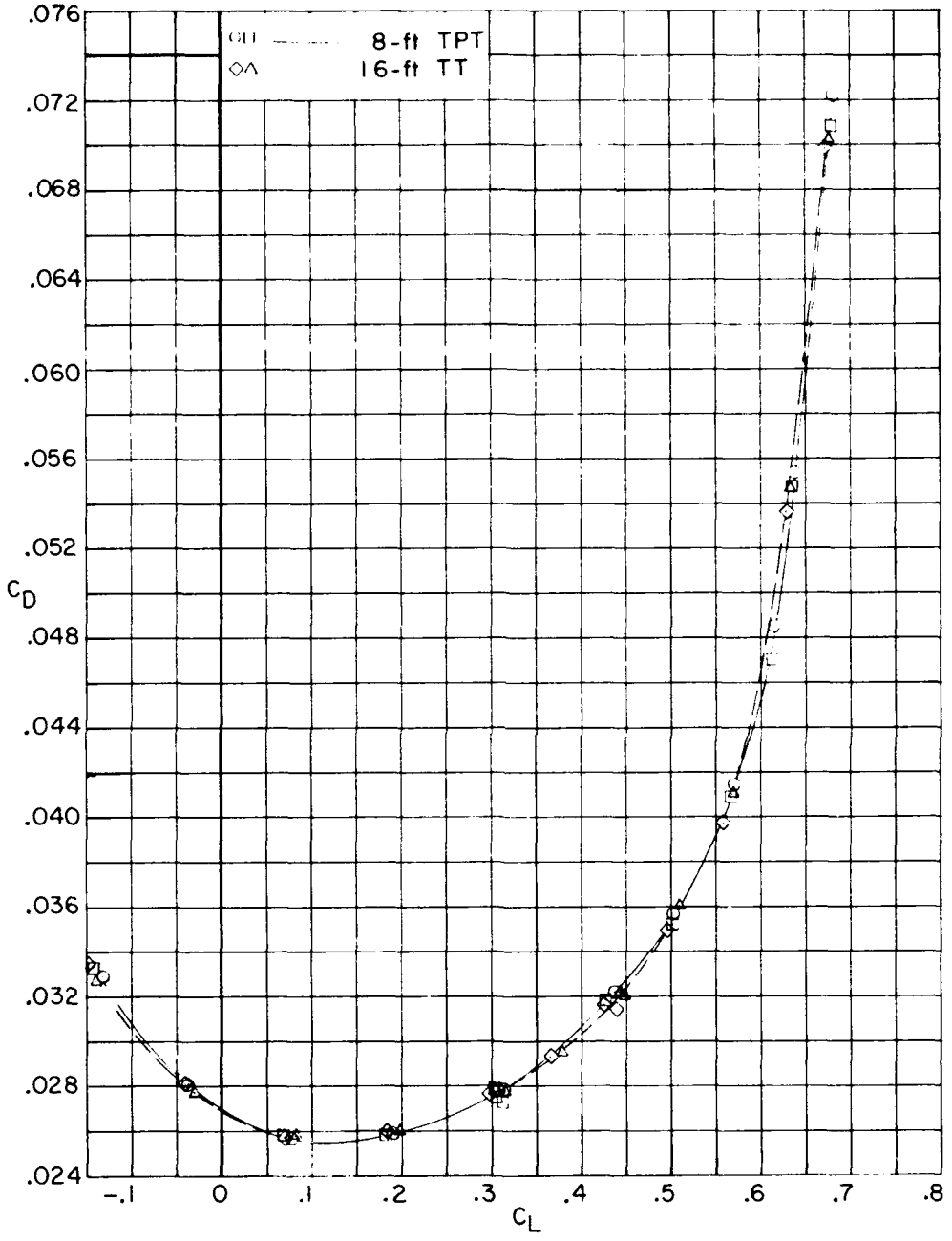

(c) M = 0.775; R = 3.5 × 10^6.

Figure 10.- Continued.

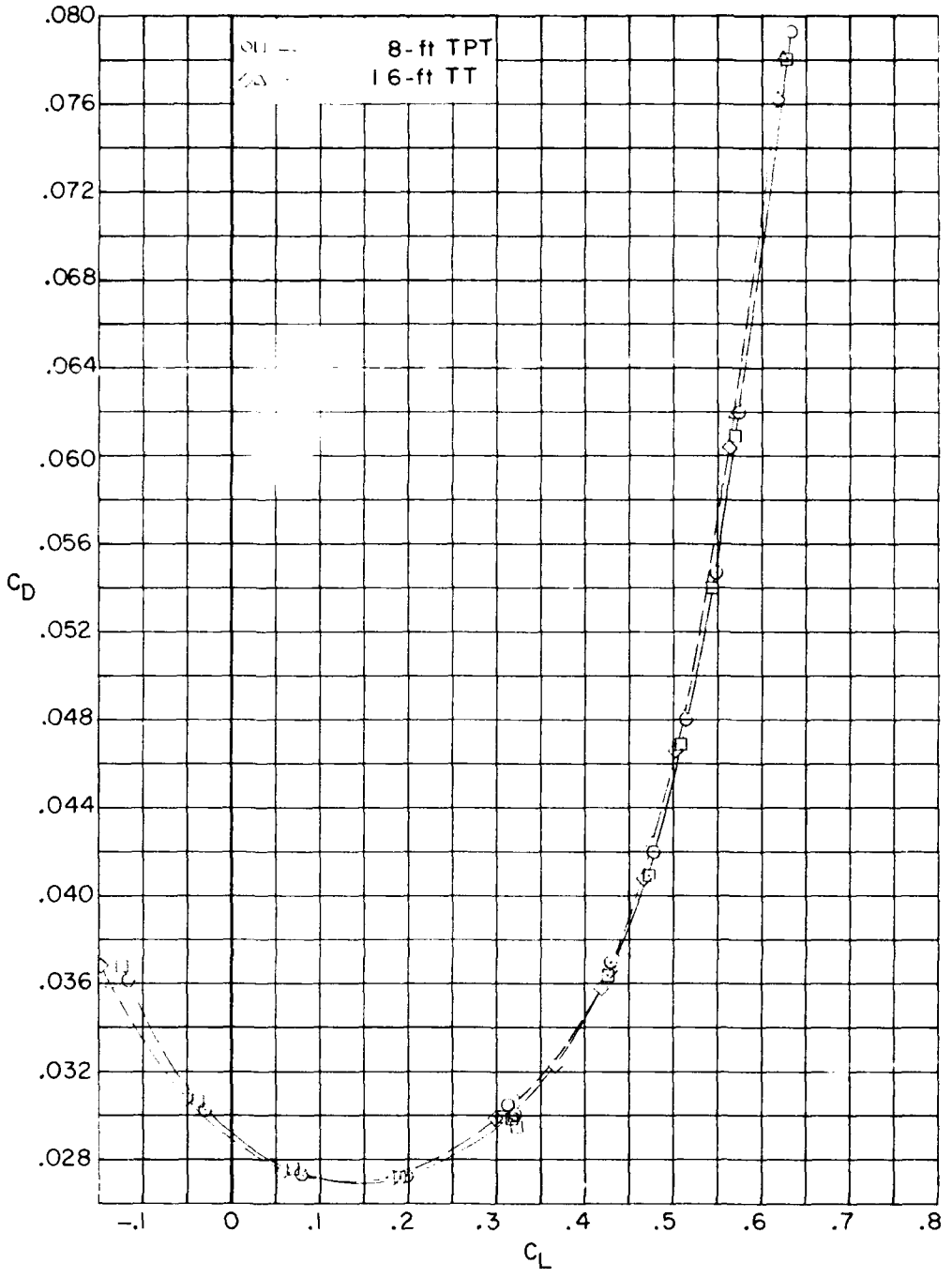

(d) M = 0.800; R = 3.5 × 10^6.

Figure 10.- Continued.

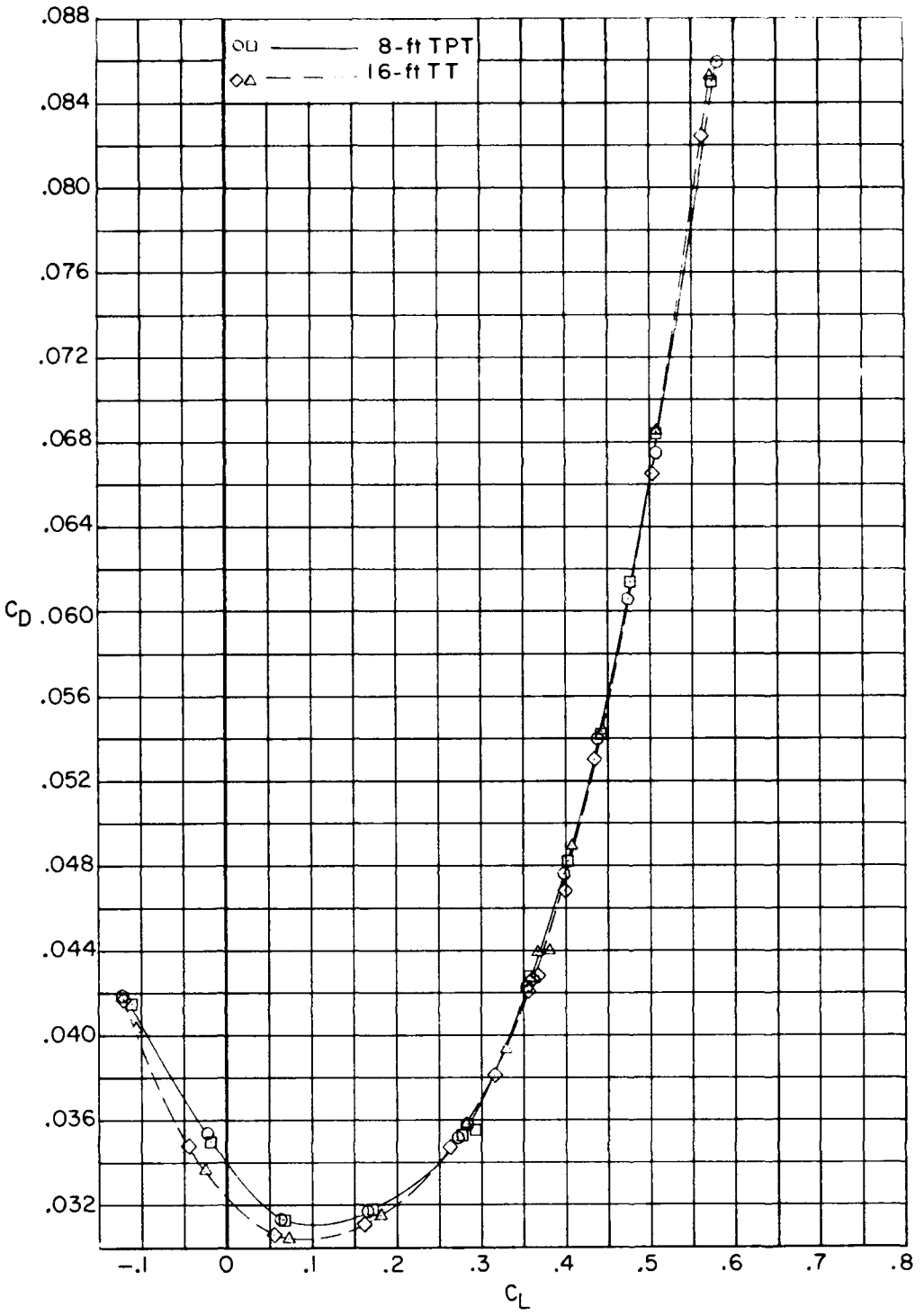

(e) M = 0.825; R = 3.6 × 10^6.

Figure 10.- Concluded.

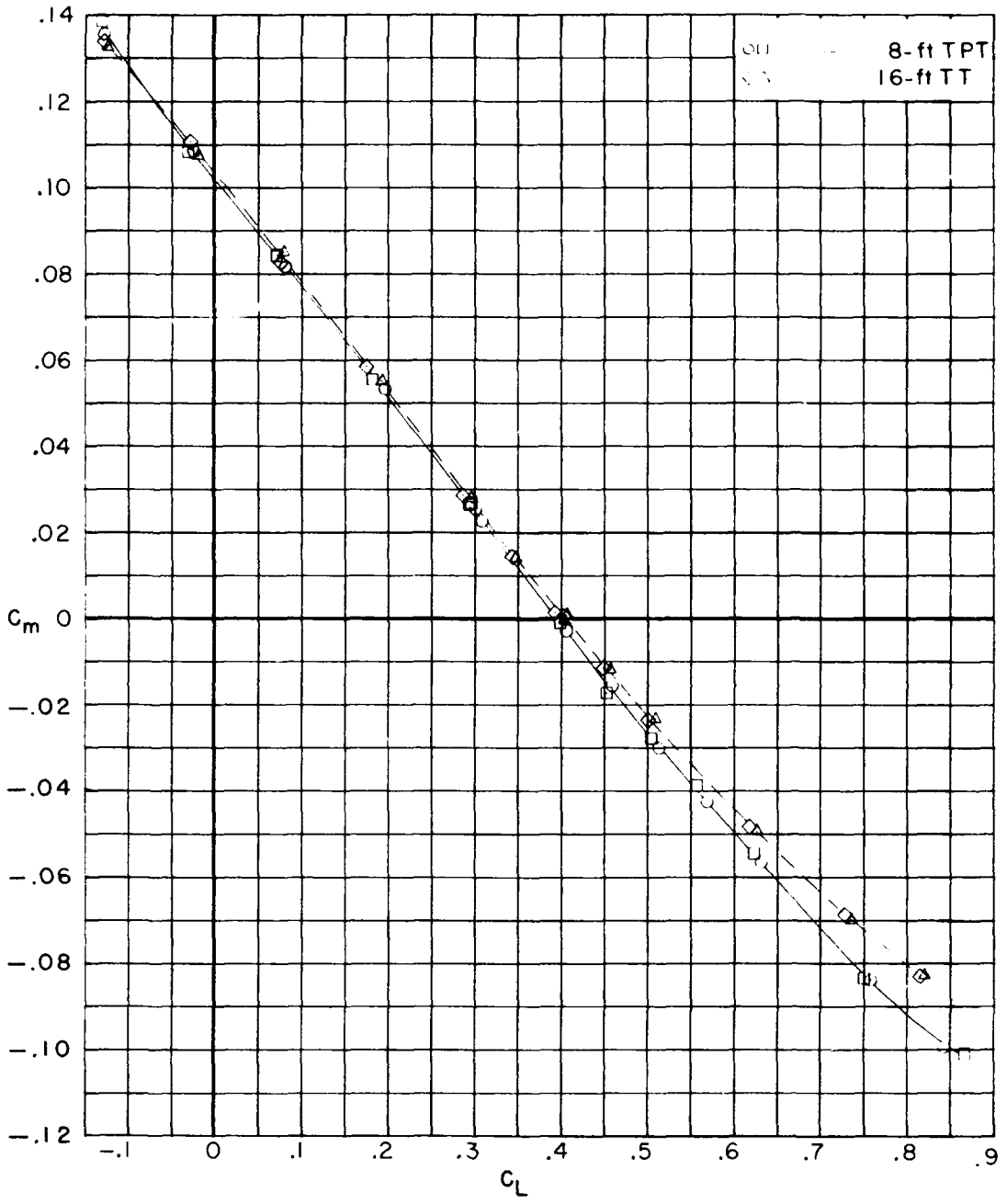

(a) M = 0.700; R = 3.3 × 10^6.

Figure 11.- Comparison of plots of pitching-moment coefficient against lift coefficient for a large subsonic cargo-type transport from tests in the Langley 8-foot transonic pressure tunnel (8-ft TPT) and in the Langley 16-foot transonic tunnel (16-ft TT). $\delta_h = 0^0$.

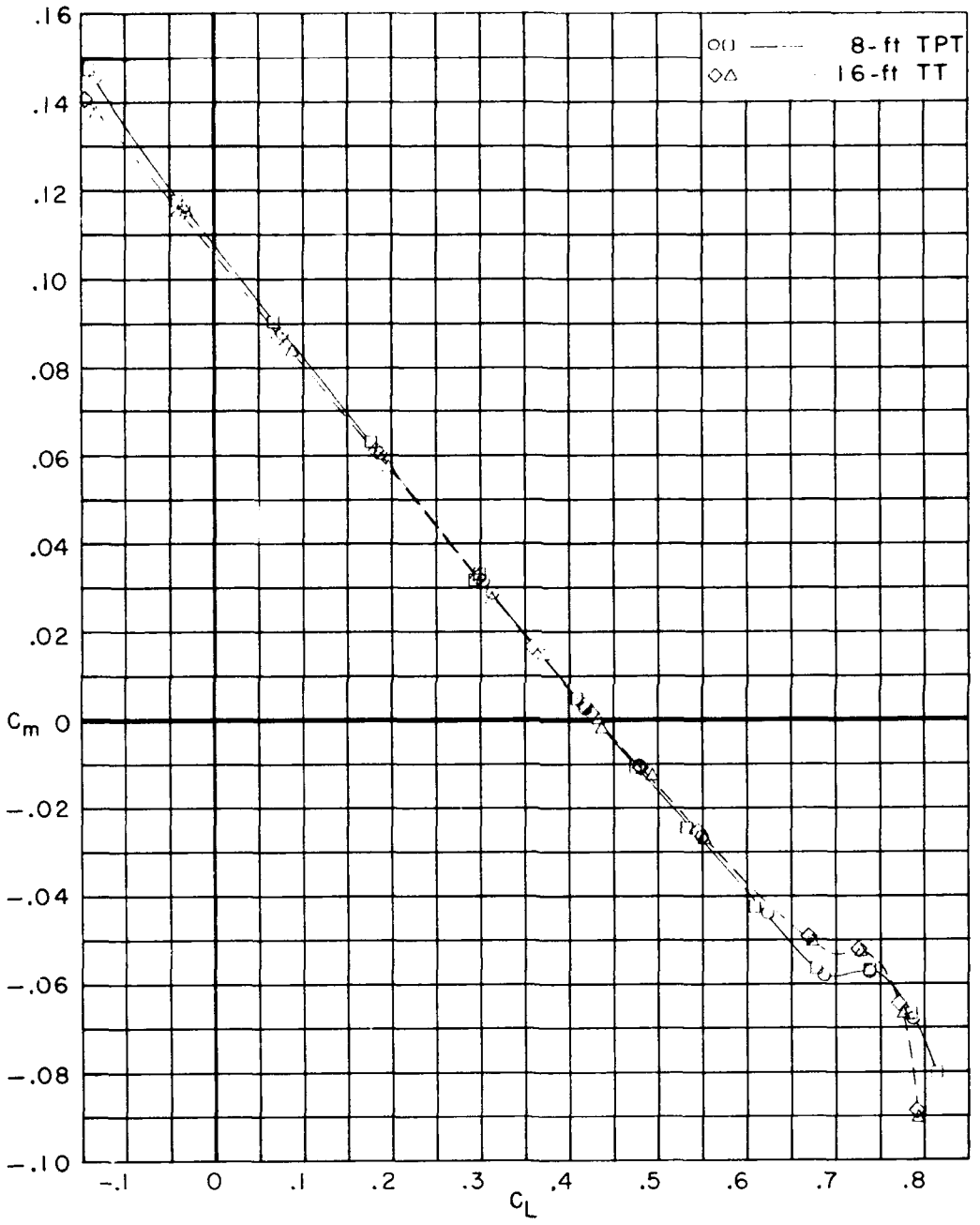

(b) M = 0.750; R = 3.4 × 10^6.

Figure 11.- Continued.

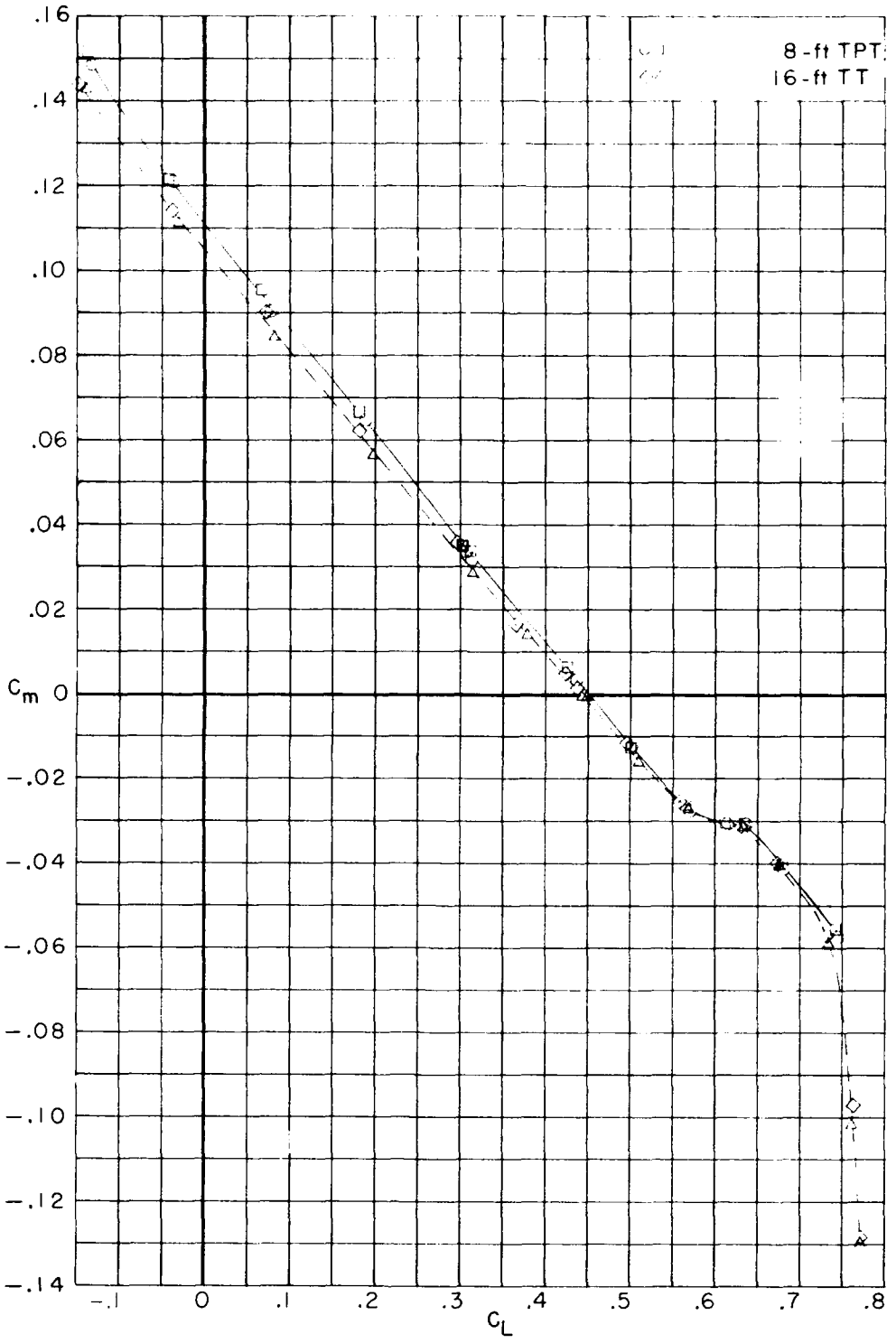

(c) M = 0.775; R = 3.5 × 10^6.

Figure 11.- Continued.

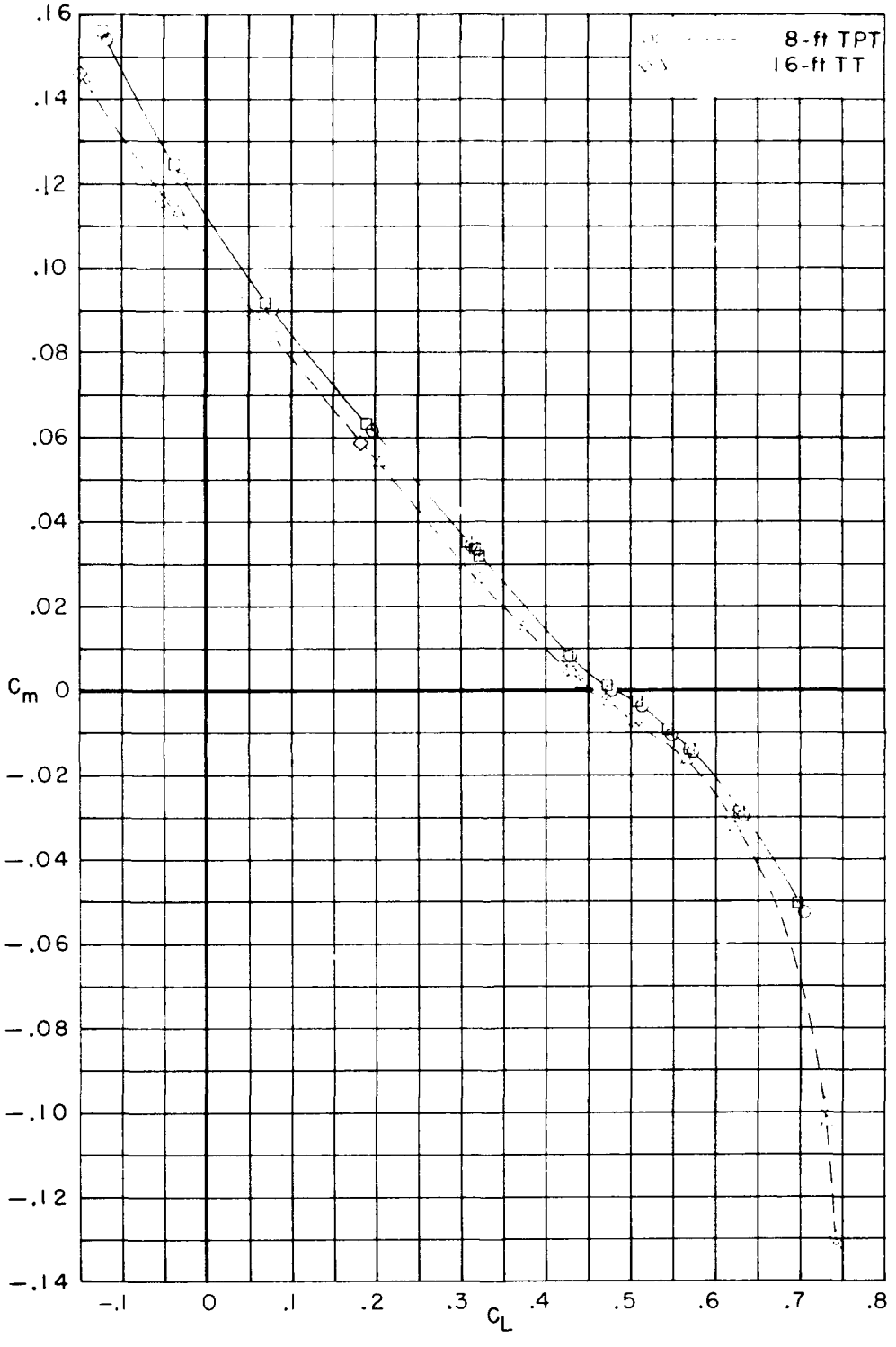

(d) M = 0.800; R = 3.5 × 10^6.

Figure 11.- Continued.

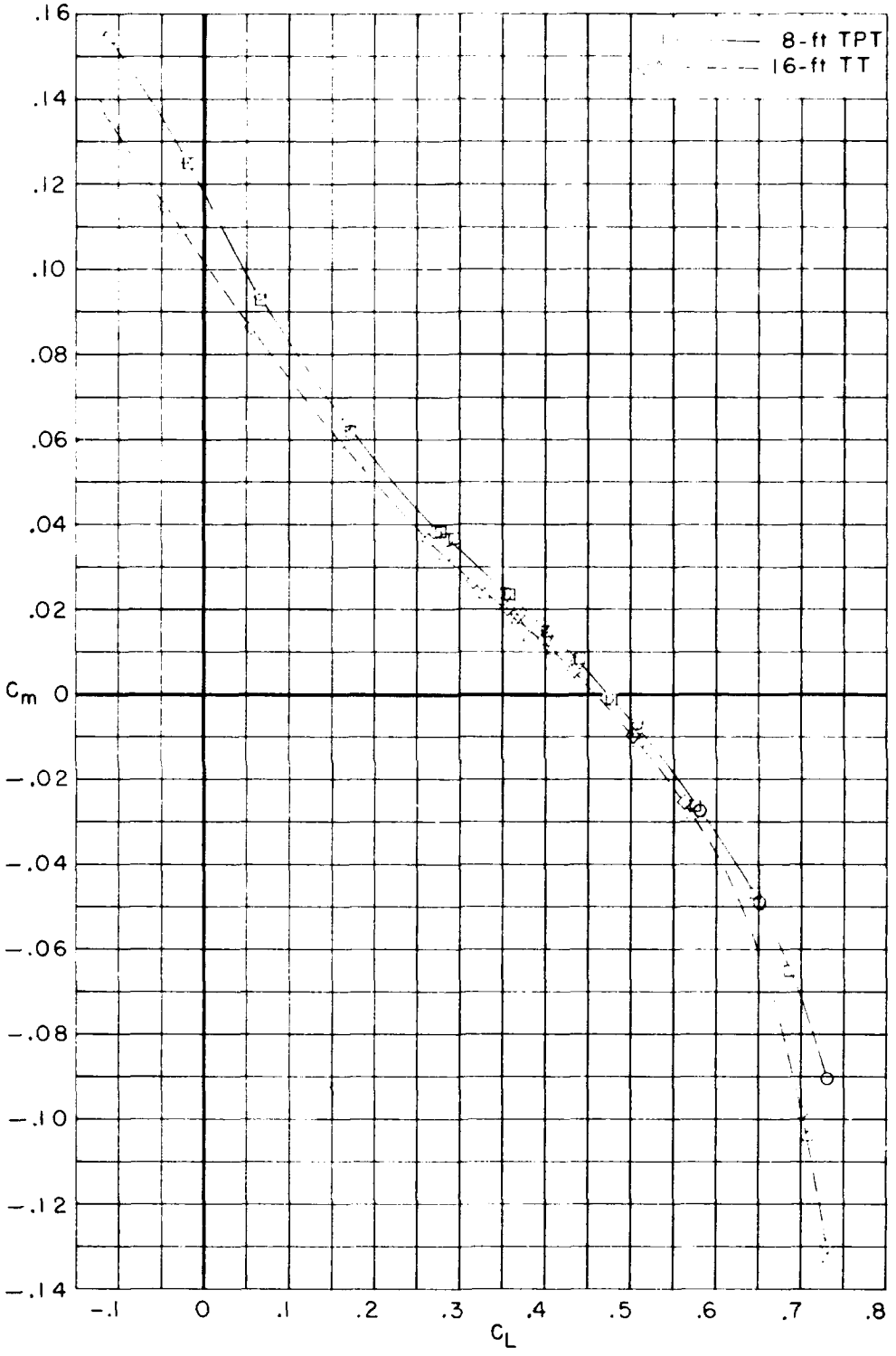

(e) M = 0.825; R = 3.6×10^6.

Figure 11.- Concluded.

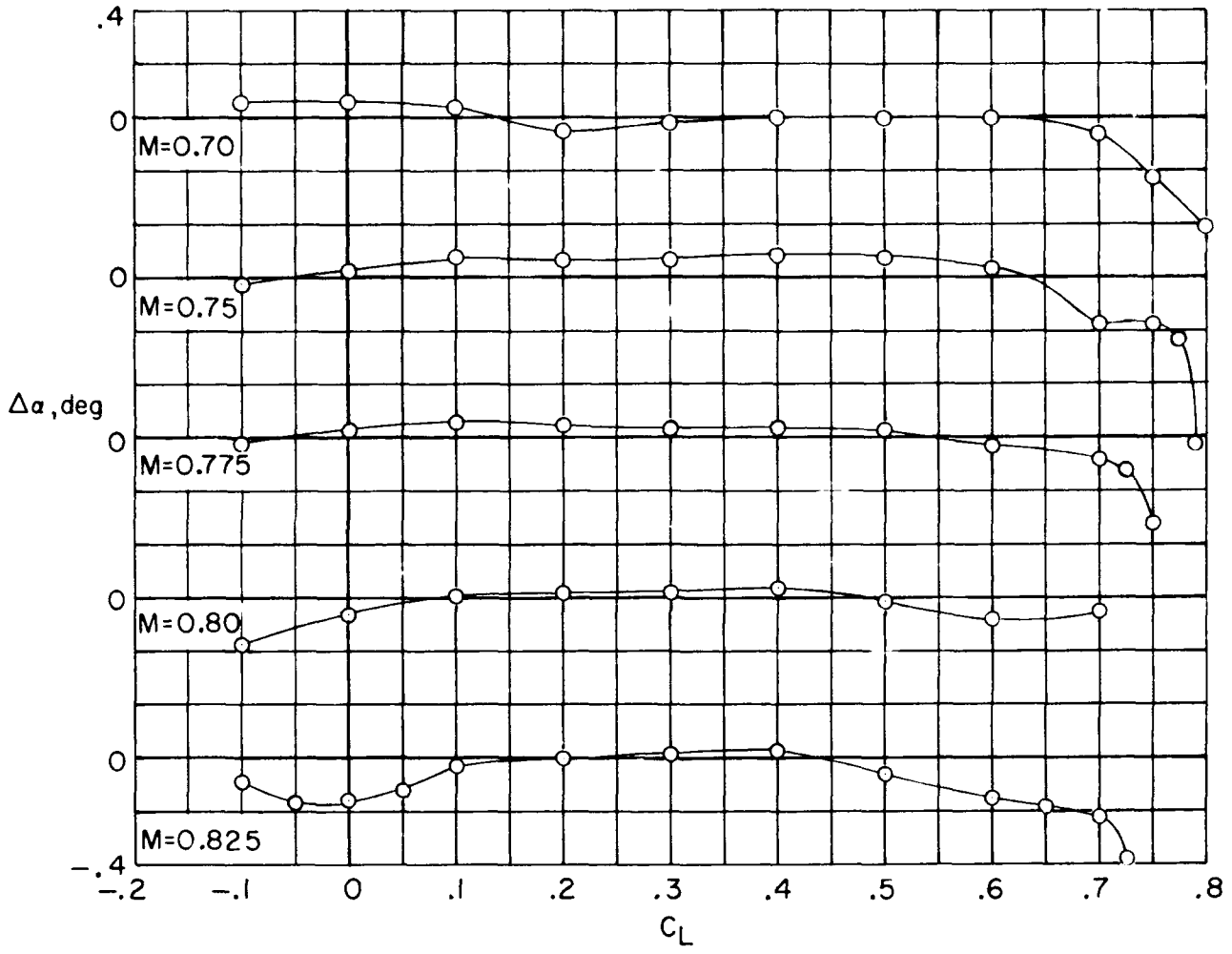

(a) $\Delta\alpha$ against C_L.

Figure 12.- Variation with lift coefficient of the difference between the Langley 8-foot transonic pressure tunnel (8-ft TPT) results and the Langley 16-foot transonic tunnel (16-ft TT) results of tests of a large subsonic cargo-type transport. $\delta_h = 0^0$; $R \approx 3.5 \times 10^6$ per foot (0.3048 m).

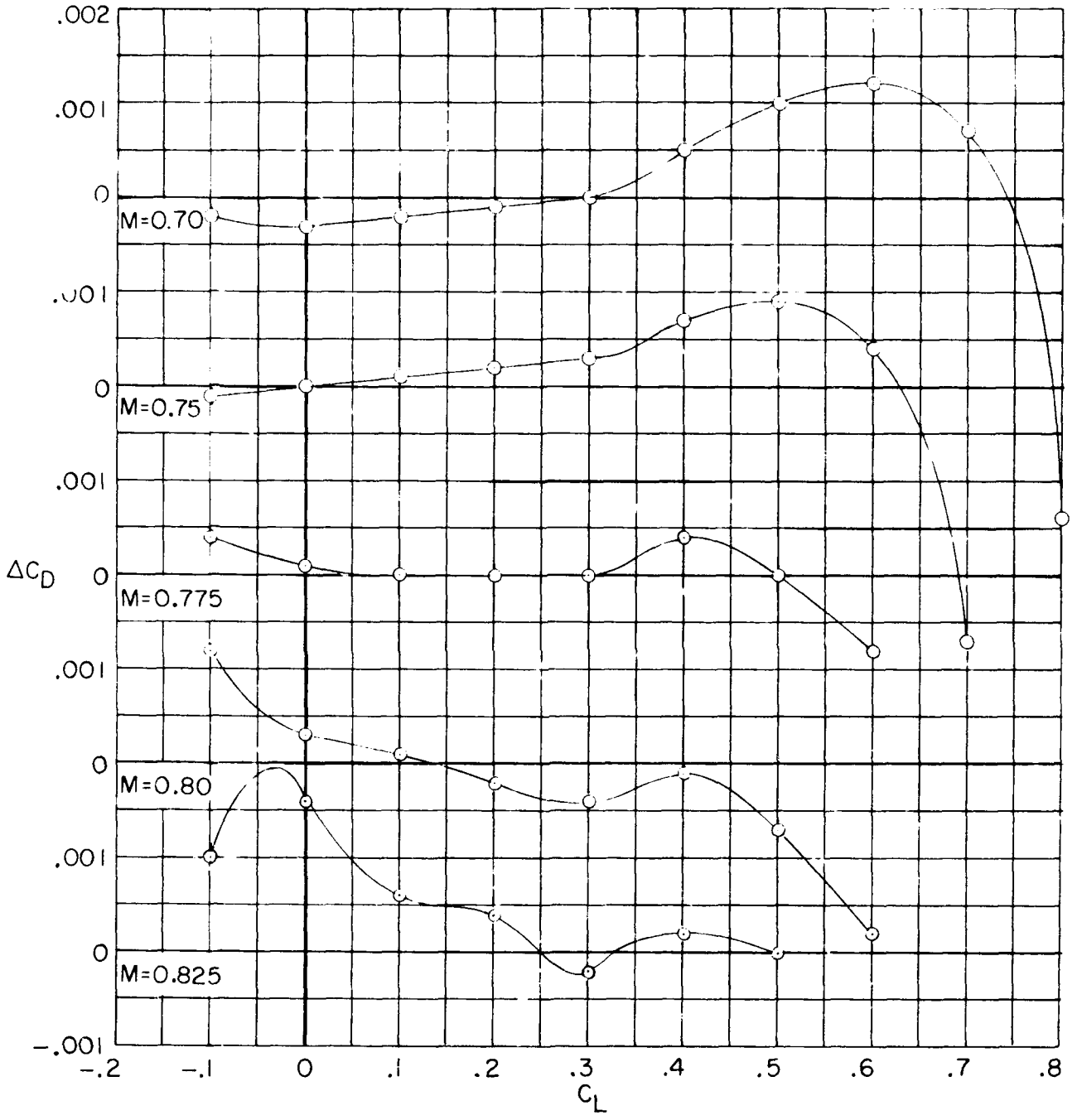

(b) ΔC_D against C_L.

Figure 12.- Continued.

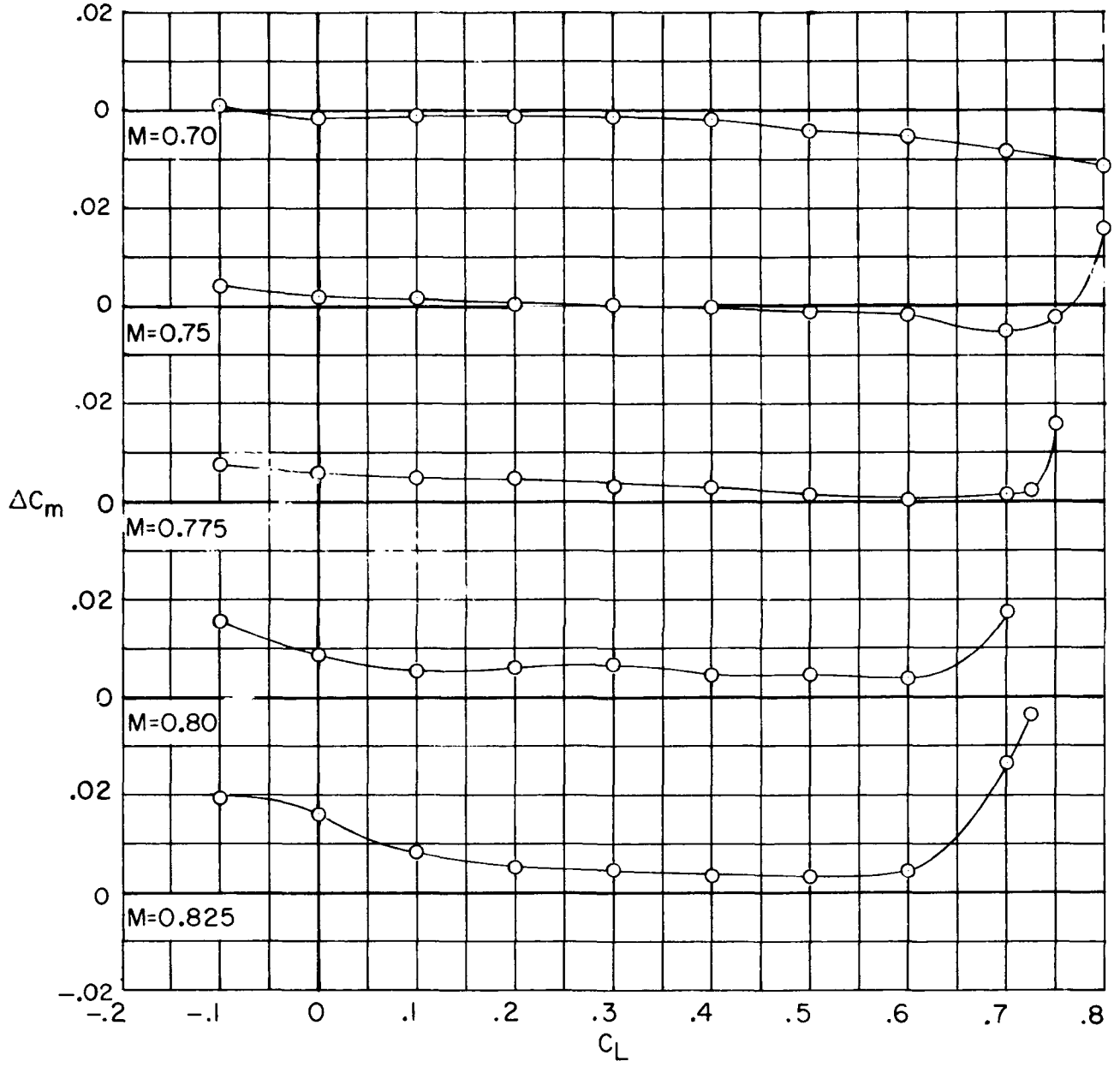

(c) ΔC_m against C_L.

Figure 12.- Concluded.

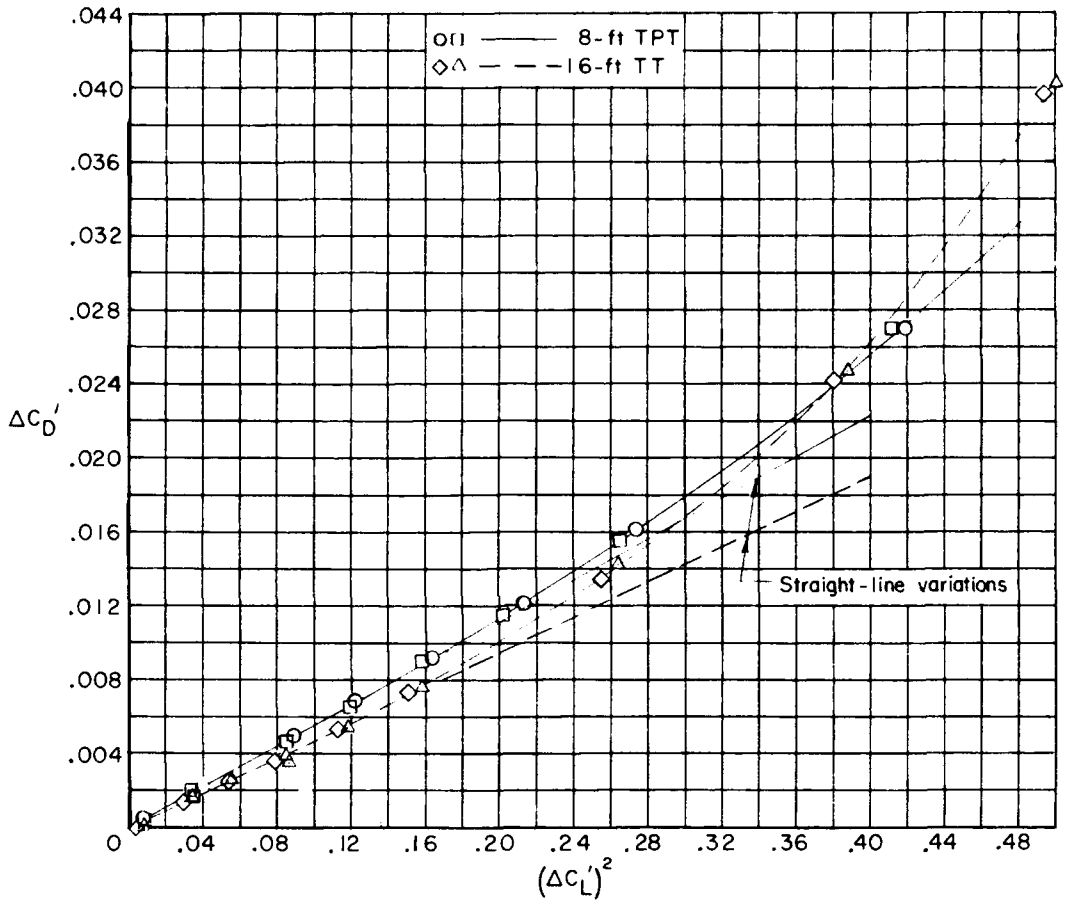

(a) $M = 0.700$; $R = 3.3 \times 10^6$.

Figure 13.- Comparison of plots of incremental drag coefficient against incremental lift coefficient squared (referenced to drag and lift at minimum-drag conditions) for a large subsonic cargo-type transport from tests in the Langley 8-foot transonic pressure tunnel (8-ft TPT) and in the Langley 16-foot transonic tunnel (16-ft TT). $\delta_h = 0^0$.

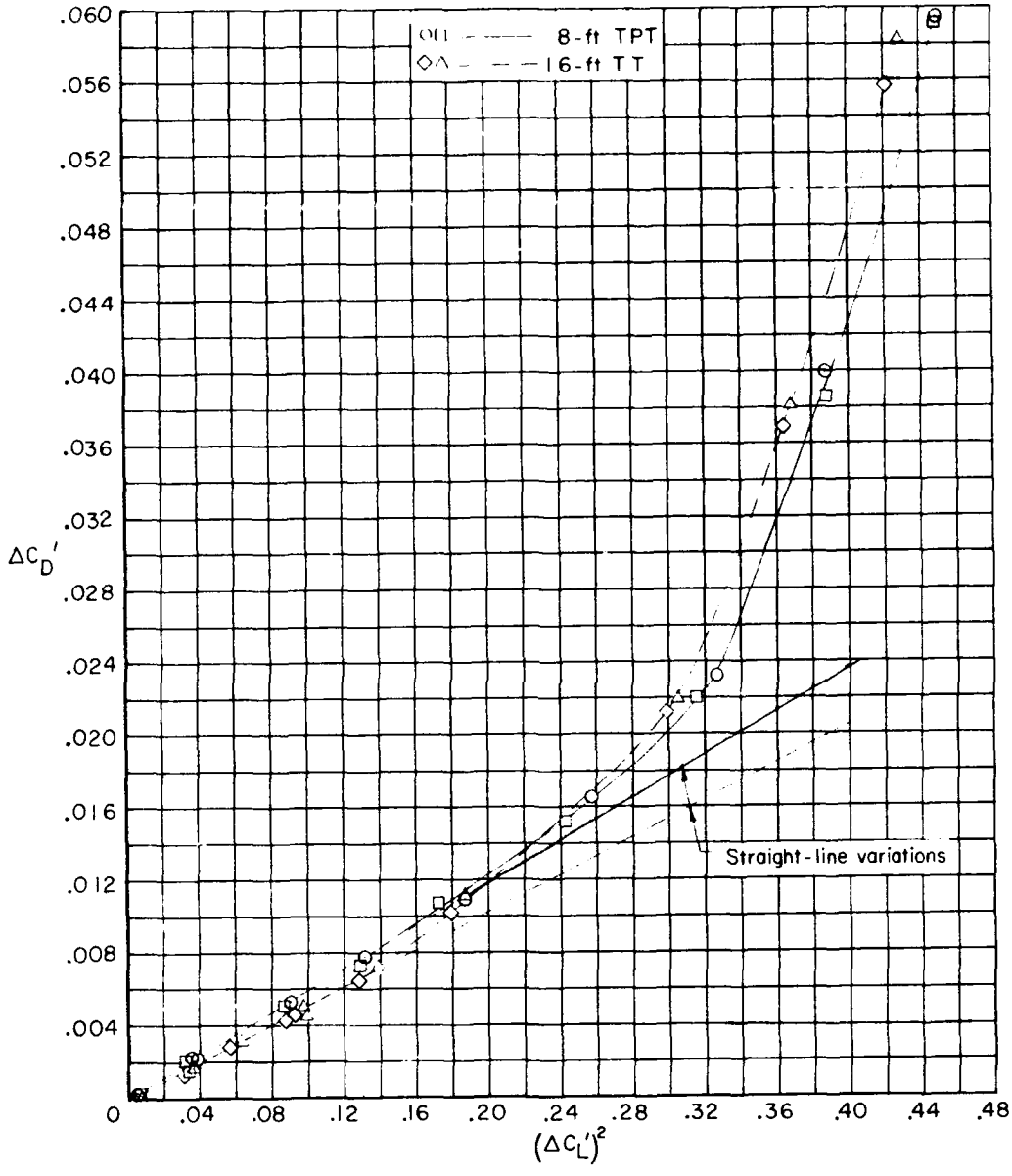

(b) M = 0.750; R = 3.4 × 10⁶.

Figure 13.- Continued.

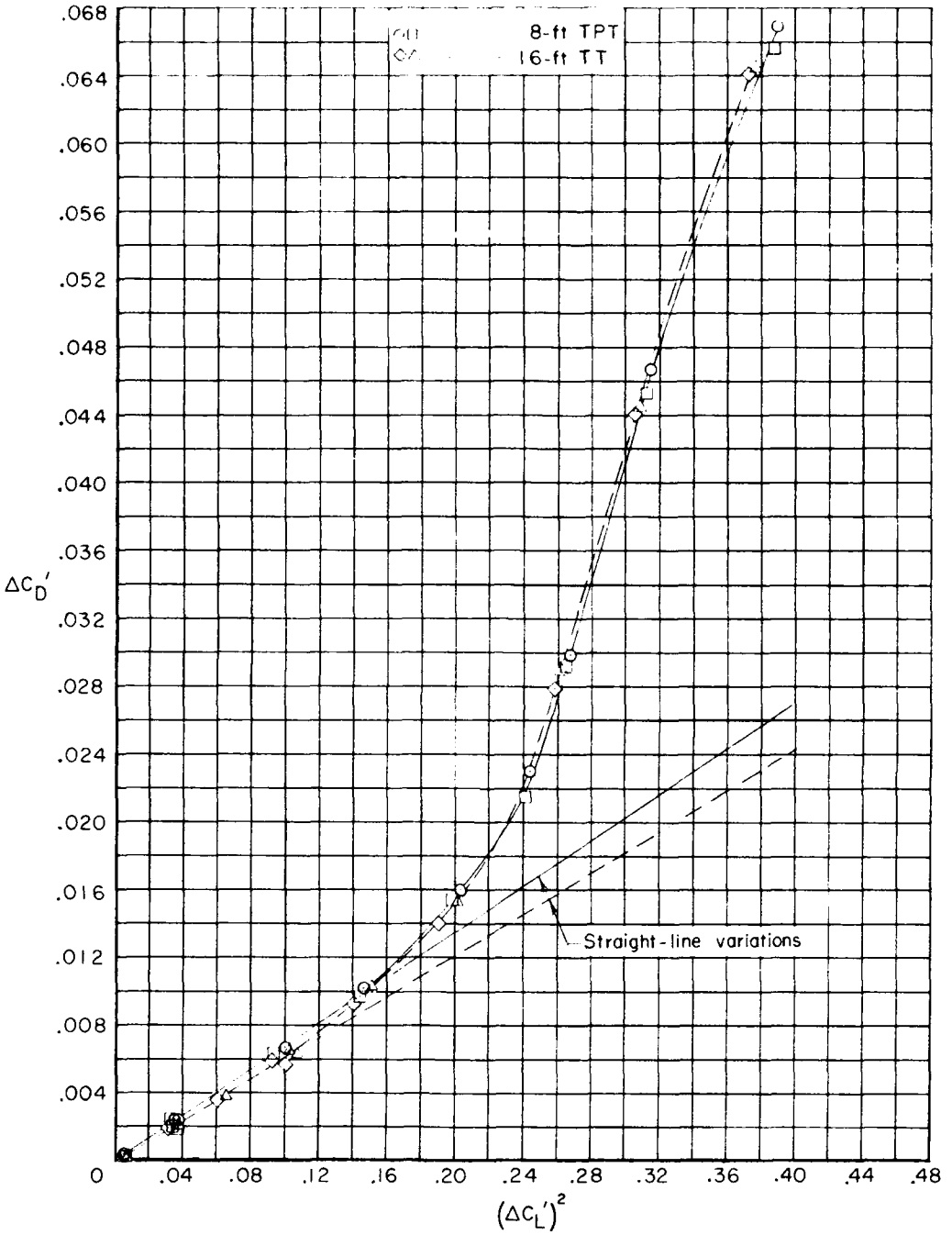

(c) $M = 0.775$; $R = 3.5 \times 10^6$.

Figure 13.- Continued.

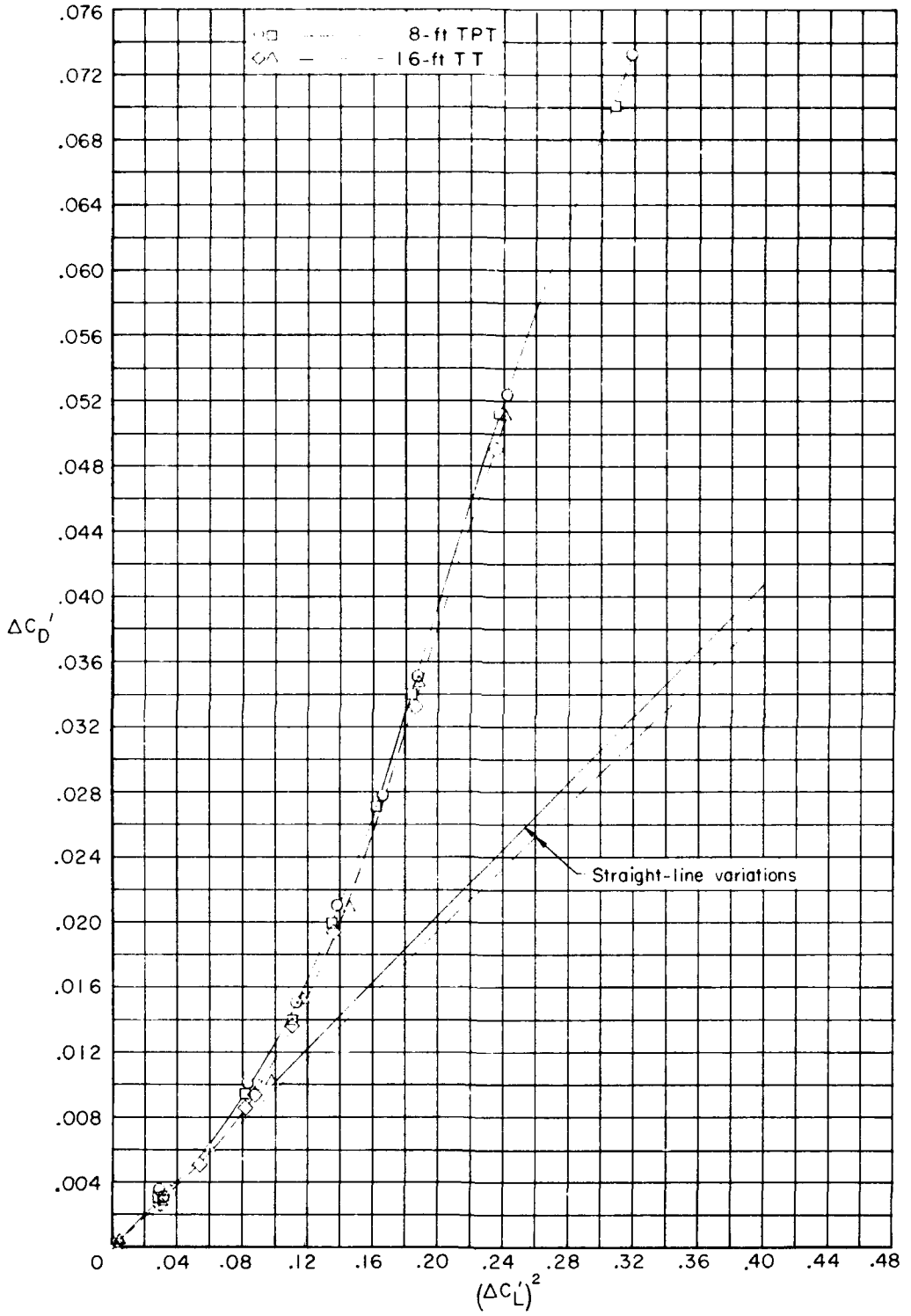

(d) M = 0.800; R = 3.5 × 10^6.

Figure 13.- Continued.

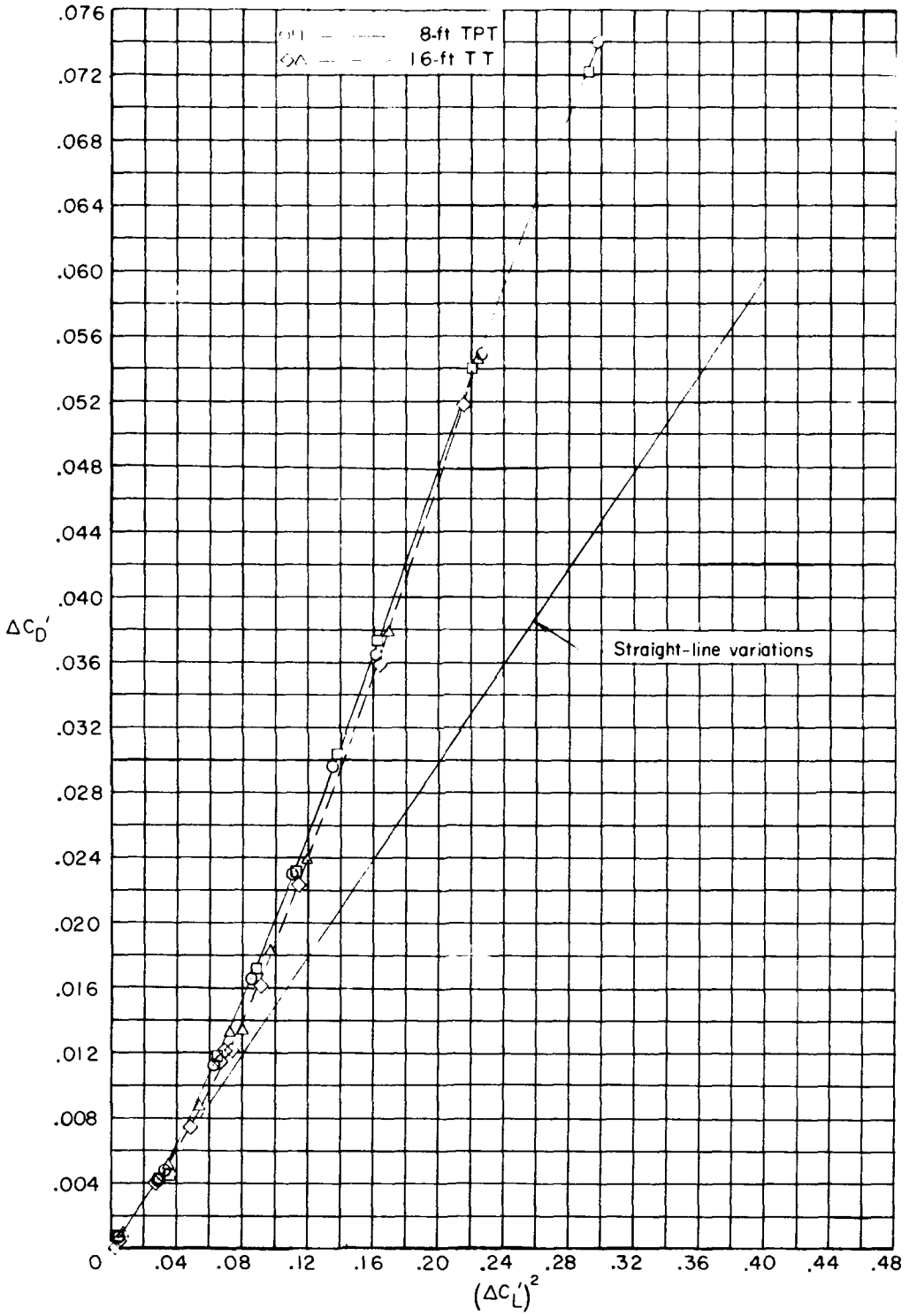

(e) $M = 0.825$; $R = 3.6 \times 10^6$.

Figure 13.- Concluded.

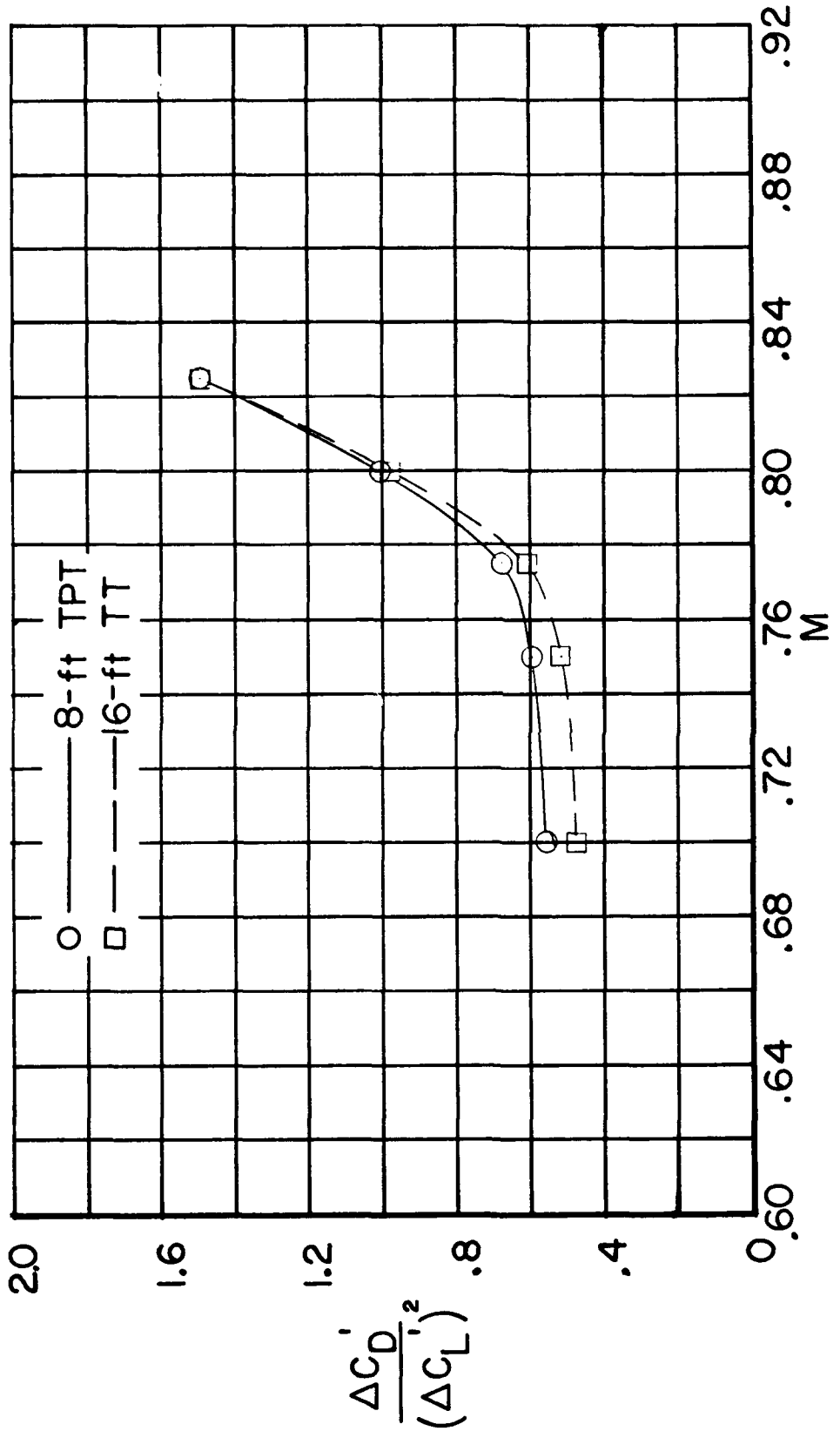

Figure 14.- Comparison of plots of drag-due-to-lift factor against Mach number for a large subsonic cargo-type transport from tests in the Langley 8-foot transonic pressure tunnel (8-ft TPT) and in the Langley 16-foot transonic tunnel (16-ft TT). $\delta_h = 0^0$; $R \approx 3.5 \times 10^6$.